

SDC mediates DNA methylation-controlled clock pace by interacting with ZTL in *Arabidopsis*

Wenwen Tian^{1,2,†}, Ruyi Wang^{1,†}, Cunpei Bo^{1,2}, Yingjun Yu^{1,2}, Yuanyuan Zhang¹, Gyeong-Im Shin³, Woe-Yeon Kim³ and Lei Wang^{1,2,*}

¹Key Laboratory of Plant Molecular Physiology, CAS Center for Excellence in Molecular Plant Sciences, Institute of Botany, Chinese Academy of Sciences, Beijing 100093, People's Republic of China, ²University of Chinese Academy of Sciences, Beijing 100049, People's Republic of China and ³Division of Applied Life Science (BK21Plus), Research Institute of Life Sciences (RILS) and Institute of Agricultural and Life Science(IALS), Gyeongsang National University, Jinju 52828, Republic of Korea

Received September 14, 2020; Revised February 13, 2021; Editorial Decision February 15, 2021; Accepted February 16, 2021

ABSTRACT

Molecular bases of eukaryotic circadian clocks mainly rely on transcriptional-translational feedback loops (TTFLs), while epigenetic codes also play critical roles in fine-tuning circadian rhythms. However, unlike histone modification codes that play extensive and well-known roles in the regulation of circadian clocks, whether DNA methylation (5mC) can affect the circadian clock, and the associated underlying molecular mechanisms, remains largely unexplored in many organisms. Here we demonstrate that global genome DNA hypomethylation can significantly lengthen the circadian period of *Arabidopsis*. Transcriptomic and genetic evidence demonstrate that *SUPPRESSOR OF drm1 drm2 cmt3* (*SDC*), encoding an F-box containing protein, is required for the DNA hypomethylation-tuned circadian clock. Moreover, *SDC* can physically interact with another F-box containing protein *ZEITLUPE* (*ZTL*) to diminish its accumulation. Genetic analysis further revealed that *ZTL* and its substrate *TIMING OF CAB EXPRESSION 1* (*TOC1*) likely act downstream of DNA methyltransferases to control circadian rhythm. Together, our findings support the notion that DNA methylation is important to maintain proper circadian pace in *Arabidopsis*, and further established that *SDC* links DNA hypomethylation with a proteolytic cascade to assist in tuning the circadian clock.

INTRODUCTION

The circadian clock allows living organisms to adjust the tempo of endogenous life processes to the daily rhythms imposed by the rotation of the earth and the earth's revo-

lution around the sun (1,2). In higher plants, the circadian clock regulates a myriad of daily and seasonal biological processes, including photoperiodic hypocotyl growth, flowering time, and biotic and abiotic stress responses (3–7). It has also been suggested that the matching between the circadian period and the external photoperiod promotes photosynthesis and enhances vegetative growth (8). Hence, it is critical for higher plants to maintain a proper circadian period to synchronize the endogenous daily rhythms with the ever-changing environmental signals (9,10).

The molecular bases of circadian clocks in many eukaryotic organisms mainly rely on transcriptional-translational feedback loops (TTFLs) (11). In *Arabidopsis*, for example, morning-expressed CIRCADIAN CLOCK-ASSOCIATED1 (*CCA1*) and LATE ELONGATED HYPOCOTYL (*LHY*) directly repress the transcription of *TIMING OF CAB EXPRESSION 1* (*TOC1*), *PSEUDO-RESPONSE REGULATOR9* (*PRR9*), *PRR7*, *PRR5*, *PRR3* and the *Evening Complex* (*EC*) components *EARLY FLOWERING 3* (*ELF3*), *ELF4* and *LUX ARRHYTHMO* (*LUX*) (12–14). Correspondingly, the transcript level of each *PRR* sequentially reaches its respective peak throughout the day, with an interval of 2–3 h from dawn to dusk. In turn, the PRR proteins subsequently repress *CCA1* and *LHY* transcription, thereby forming multiple TTFLs (15–17). In addition to TTFLs, core clock components are maintained at the post-translational level by ubiquitination-mediated proteasomal degradation. For example, the F-Box protein *ZEITLUPE* (*ZTL*) promotes the 26S proteasome-dependent degradation of *TOC1* and *PRR5* proteins in the darkness to keep the rhythm robust (18,19). Interestingly, the *ZTL* protein itself also oscillates, although its transcript level is constant at different time points during the day. Importantly, mutation or mis-expression of any core clock component at either the transcriptional or post-transcriptional level signifi-

*To whom correspondence should be addressed. Tel: +86 10 62836175; Email: wanglei@ibcas.ac.cn

†The authors wish it to be known that the first two authors should be regarded as Joint First Authors.

cantly alters the circadian clock, and even abolishes overt rhythmicity under free-running conditions (20).

Epigenetic codes play critical roles in gene regulation (21–24). In addition to histone modification, the other epigenetic code, genomic cytosine methylation (5mC), is generally thought to cause chromatin compaction and gene expression alteration, which contributes to trait variation in a range of eukaryotic organisms (25). The 5mC homeostasis reflects dynamic regulation among its establishment, maintenance and removal in plants and animals (25,26). The 5mC methylation in mammals occurs virtually exclusively in the CG context (27); its maintenance is via DNA METHYLTRANSFERASE 1 (DNMT1) (28). DNA CG methylation status of *BMAL1* and *PERIOD 2* (*PER2*), two core components of the mammalian circadian clock, are associated with obesity, metabolic syndrome, and weight loss (29). In addition, the DNA hypermethylation of the CG island of the *BMAL1* promoter reduces its expression and prohibits the recruitment of CLOCK proteins to their common targets, disrupting the cellular circadian clock and thereby contributing to the development of hematologic malignancies (30). Maintenance of 5mC in higher plants is through distinct mechanisms depending on the cytosine contexts, namely CG, CHG and CHH (H denotes A, T or C) (31,32). The CG methylation is majorly maintained by DNA METHYLTRANSFERASE 1 (MET1) (33), while the CHG site is methylated by CHROMOMETHYLASE 3 (CMT3) and CMT2 in a redundant manner (34,35). In addition, CMT2 preferentially methylates CHH sites (36), and together with DOMAINS REARRANGED METHYLTRANSFERASE 2 (DRM2) maintains CHH methylation (26,32,34). DNA cytosine methylation controls many key developmental processes in higher plants such as flowering transition, immune response, and fruit ripening (37–41). Loss of CG DNA methylation in *met1* produces the late flowering phenotype in *Arabidopsis*, mainly through affecting *FLOWERING WAGENINGEN* (*FWA*) expression (42), while plants with a deficiency of the majority of non-CG DNA methylation in *drm1 drm2 cmt3* triple mutants displayed curled leaves and reduced stature phenotypes; this is considered to be due to *SUPPRESSOR OF drm1 drm2 cmt3* (*SDC*) promoter demethylation (43). However, whether DNA methylation is involved in the regulation of the circadian clock in higher plants, and the associated underlying molecular mechanisms, remain largely unknown.

In this study, we found that pharmacologically or genetically reducing the global genomic cytosine methylation level resulted in a significantly lengthened circadian period in *Arabidopsis*. Furthermore, we identified SDC to mediate DNA hypomethylation controlled circadian rhythms. Moreover, SDC physically interacted with the ZTL protein to compromise its stability which might lead to de-repression of TOC1, a substrate of ZTL. Collectively, our findings indicate that DNA methylation is a new cellular parameter mediated by SDC involved in the proteolytic cascade to fine-tune the circadian clock.

MATERIALS AND METHODS

Plant materials and plasmid construction

For seedling growth, *Arabidopsis* seeds were sterilized and plated on MS (Murashige-Skoog) plates with 3% sucrose

and 0.7% agar. After stratification for three days at 4°C, the plates were transferred to a growth chamber with a 12-h light/12-h dark photoperiod at 22°C. *Arabidopsis* mutant *drm1-2 drm2-2 cmt3-11t* (*ddc3*), *cmt2-3*, and *sd* were ordered from Arabidopsis Biological Resource Center (ABRC, the Ohio State University). To generate the *drm1-2 drm2-2 cmt2-3 cmt3-11t* (*ddc2c3*) quadruple mutant, the homozygous *drm1-2 drm2-2 cmt3-11t* mutant was genetically crossed with the *cmt2-3* mutant. The homozygous F2 plants of *drm1-2 drm2-2 cmt2-3 cmt3-11t* were self-pollinated to obtain F3 progeny seeds for further assay. For the real-time luminescence assay, the above mutants were respectively crossed with *CCA1:LUC* or *LNK2:LUC* reporter lines. After PCR-based scoring, F3 homozygous plants were used for a circadian phenotype assay. To analyze the circadian phenotype of the *met1-3* mutant, it was crossed with *CCA1:LUC* reporter line. F2 progeny seedlings were used for imaging. After PCR-based scoring, the homozygous *met1-3* and WT seedlings with circadian reporters segregated from the same F2 seed pool were used to analyze their respective circadian phenotypes. The mutants used for circadian period analysis are listed in Supplementary Table S1.

To construct *35S:GFP-SDC* and *35S:GFP-ZTL* vectors, their respective full length coding sequence (CDS) fragments were subcloned into the *Kpn* I and *Xho* I sites of the *pENTR2B* vector and then recombined to the *pMDC45-GFP* vector using Gateway LR Clonase enzyme mix (Invitrogen) (24). To generate the *CsVMV:SDC-HA* and *CsVMV:FKF1-HA* vector, the full length *SDC* and *FKF1* fragments were subcloned into the *Kpn* I and *Xma* I, *Pac* I and *Kpn* I sites of the *pCsVMV-HA3-N-1300* vector, respectively (24). To construct the *35S:ZTL-FLAG* vector, the full-length *ZTL* fragment was amplified and then subcloned into the *Spe* I and *Kpn* I sites of the *p35S-FLAG-1307* vector (44). The *SDC* overexpression transgenic lines were generated by *Agrobacterium*-mediated transformation of *pCsVMV-SDC-HA* or *35S:GFP-SDC* by floral dipping. After confirmation by protein immune blotting and RT-qPCR, the independent T1 transgenic plants were screened, and the lines with a 3:1 segregation ratio were self-pollinated to obtain homozygous plants for further study. The primers used for constructs and RT-qPCR are listed in Supplementary Table S2.

Luminescence real-time measurement and circadian rhythm analysis

Arabidopsis seeds of Col-0 wild type and the indicated mutants harboring *CCA1:LUC*, *LHK2:LUC* or *CAB2:LUC* reporters were sterilized and plated on MS plates for stratification about three days at 4°C. The plants were grown in 12-h light/12-h dark and 22°C for eight days and were then transferred to MS plates with or without DNA methyltransferase inhibitors 5-Aza-dC (20 or 40 mg/l) or Zebularine (100 mg/l) for circadian phenotype analysis under constant red (LED light bulbs producing 660 nm wavelength for photon irradiance, light intensity 40 μmol/m²/s) or blue light (LED light bulbs producing 470 nm wavelength photon irradiance, light intensity 40 μmol/m²/s) at 22°C as noted. Luminescence intensity derived from luciferase activity was determined using a CCD camera (LN/1300-EB/1, Princeton Instruments) as previously described (5). Luminescence

image acquisition was conducted for up to 144 h with 20 min exposure time and 2-h intervals.

Statistical analysis of bioluminescence data

The time course of bioluminescence intensity was analyzed using MetaMorph Microscopy Automation and Image Analysis Software. Bioluminescence data were imported into the Biological Rhythms Analysis Software System (BRASS v2.14, available from www.amillar.org) to calculate period lengths from individual traces using the Fourier transform-nonlinear least-squares suite of programs. Data were presented as mean \pm SEM and were analyzed by the independent-samples *t*-tests when comparing two groups, or one-way ANOVA followed by Fisher's LSD test for comparing more than two groups.

RNA extraction and quantitative RT-PCR

After stratification under 4°C for three days, the *Arabidopsis* seedlings were grown in 12-h light/12-h dark at 22°C for 8 or 10 days as noted. The samples were collected at the indicated time points for RNA extraction. For the infiltrated leaves of *N. benthamiana*, the samples were harvested as indicated. For testing the transcript level, total RNA was extracted with TRIzol reagent (Invitrogen). One microgram of RNA was used for DNA removal and reverse transcription, and cDNA synthesis was performed using a PrimeScript® RT reagent Kit (TaKaRa) as according to the manufacturer's instructions (7). Quantitative PCR was conducted with Real-time PCR SYBR Green Master Mix (Toyobo, Japan). Specific gene transcription abundance was normalized according to *ACTIN2* and *TUB4* transcription expression. The gene-specific primers listed in Supplementary Table S2 were used for the quantification of corresponding mRNA levels via quantitative RT-PCR using the Applied Biosystem Quant Studio 3 detection system. To examine the effect on the circadian period by 5-Aza-dC using time-course RT-qPCR, *Arabidopsis* Col-0 seedlings were grown on MS plates in 12-h light/12-h dark for eight days and then were transferred to MS plates in the absence or presence of 20 mg/l 5-Aza-dC under constant light conditions. Samples were collected from LL48 h to LL116 h at 4-h intervals under constant light conditions. RNA extraction and quantitative RT-PCR were performed to measure the transcript levels of *CCA1* and *LHY* in a time-course manner.

Bimolecular fluorescence complementation (BiFC) assays

For the BiFC assay, the coding sequences of the 21 functional identified circadian genes were cloned into *Pac I* and *Spe I* sites of a 2YC-pBI-cYFP vector using ClonExpressTM (Vazyme, China). *SDC* was cloned into the 2YN-pBI-nYFP to obtain *SDC-nYFP* vector (24). *N. benthamiana* leaves were co-infiltrated with *Agrobacterium* containing the indicated plasmid combination. H2B-mCherry was used as a nuclear-localization marker. The fluorescence signal was detected at 72 h after agroinfiltration with an Olympus FV1000 MPE confocal microscope.

GST pull down assays

The full-length *SDC* coding region was fused to a GST tag with *Bam* HI and *Xho* I sites to produce the *GST-SDC* construct. The plasmid was transformed into *Escherichia coli* BL21 strain, and the GST-SDC protein was induced with 1 mM IPTG at 30°C for 3 h and then purified with glutathione-agarose (Sigma, USA) according to the protocol described (45). The purified GST and GST-SDC beads were incubated with an equal amount of *N. benthamiana* leaves expressing ZTL-FLAG or FKF1-HA protein extracts. After washing as a previous method (46), GST proteins were analyzed by SDS-PAGE and Coomassie Brilliant Blue R250 staining. Pulled-down proteins were detected by immunoblotting using FLAG antibody (M20008, Abmart) or HA antibody (11867423001, Roche, Switzerland) as noted.

Co-immunoprecipitation (Co-IP) assays

Co-IP assays were performed by agroinfiltration-based transient expression of GFP-SDC/ZTL-FLAG or GFP-SDC/FKF1-HA combination in 5-week-old *N. benthamiana* leaves. Samples were collected after three days, and total proteins were extracted using ice-cold protein extraction buffer (50 mM Tris-Cl, pH 7.5, 150 mM NaCl, 0.5% Nonidet P-40 (v/v), 1 mM dithiothreitol, 1 mM EDTA, 1 mM phenylmethylsulfonyl fluoride, 2 mM Na₃VO₄, 2 mM NaF, 1 µg/ml aprotinin, 1 µg/ml Pepstatin A, 5 µg/ml Leupeptin, 5 µg/ml Antipain, 5 µg/ml Chymostatin, 50 µM MG132, 50 µM MG115, 50 µM ALLN) (47). Immunoprecipitation was carried out with GFP-Trap beads (GTMA-20-20rxns, Chromo Tek). Three microliters of the input and 10 µl of the Co-IP sample (SDS loading buffer added) were loaded. GFP-tagged SDC, FLAG tagged ZTL and HA tagged FKF1 proteins were fractionated by 10% SDS-PAGE (acrylamide: bisacrylamide, 37.5:1) gels. Immunoblotting was performed using a 1:2000 dilution of the primary polyclonal anti-GFP antibody (Abcam ab6556), a 1:2000 dilution of the monoclonal primary anti-Flag antibody (Abmart, M20008) or 1:1000 monoclonal primary anti-HA antibody (Roche, 11867423001). The 1:3000 HRP-linked anti-rabbit IgG, anti-mouse IgG or anti-rat IgG were used as secondary antibodies accordingly. Chemiluminescence reactions were performed with Supersignal west pico chemiluminescent substrates (Thermo Fisher Scientific, 34580EA).

RNA-sequencing analysis

For the DNA methyltransferase inhibitor treatment, *Arabidopsis* Col-0 seedlings were grown under 12-h light/12-h dark conditions and 22°C on the MS plates for nine days and were then transferred to plates containing 40 mg/L 5-Aza-dC or an equal volume of DMSO solution. The treated seedlings were collected at ZT1 and ZT13 of the next day for RNA extraction. For RNA-sequencing with the *ddc2c3* quadruple mutants, the seedlings were grown under 12-h light/12-h dark conditions and 22°C for 8 days and then transferred to constant white light conditions. Samples were collected at LL24 and LL36.

Total RNA was extracted with TRIzol reagent (Invitrogen) and treated with DNase I (Thermo Fisher). RNA quality was assessed using the RNA Nano 6000 Assay Kit of the Bioanalyzer 2100 system (Agilent Technologies, CA, USA) and Qubit® RNA Assay Kit in Qubit® 2.0 Fluorometer (Life Technologies, CA, USA). For 5-Aza-dC treatment, both the RNA-sequencing and differential gene expression analyses were performed by RedtreeTech Inc. For RNA-seq of Col-0 and *ddc2c3* at LL24 and LL36, the sequencing were performed on Illumina Nova-seq platform with paired-end 150 bp at BerryGenomics (Beijing, China). The analysis was performed on a commercial server in which computational pipelines was pre-established (8 omics Gene Technology Co. Ltd, Beijing, China). The details for RNA-Sequencing and differential gene expression analyses were as previously described (7,45). RNA-seq raw data have been deposited in the Gene Expression Omnibus database under accession number GSE153510. The sequence tracks can be accessed at public sessions (<http://genome.ucsc.edu/cgi-bin/hgPublicSessions>) by manually searching with either genome assembly name ‘hub_329263.araTha1’ or session name ‘Mechanism of 5mC controlled Arabidopsis clock pace’, and the processed data in bigwig format were deposited to github (<https://github.com/Yuanyuanzhang-IBCAS/Transcriptomedata.git>). The source code for differential expression genes analysis was deposited to github (<https://github.com/Yuanyuanzhang-IBCAS/source-code-for-Mechanism-of-5mC-controlled-Arabidopsis-clock-pace.git>). Meanwhile, the python packages, modules, software, scripts and configuration files were deposited to Zenodo (10.5281/zenodo.4435146, https://zenodo.org/record/4435146#.X_5ISxmpS71). All the experimental results were validated critically step by step by the company including RNA quality control, libraries size and reads quality, and the RNA-seq data were validated using RT-qPCR.

Hypocotyl length measurements

Arabidopsis seeds were sown on MS medium containing 1% sucrose and stratified at 4°C for 3 days. Then, the plates were transferred to 12-h light/12-h dark conditions to grow for an additional 5 days. The hypocotyl length was measured with ImageJ software (48).

ZTL Protein degradation assay in planta

To obtain the *CsVMV:ZTL-LUC* fusion vector, a *LUCIFERASE (LUC)* fragment was cloned into a *pCsVMV-1300* vector with *Xma* I and *Nco* I sites, and then a *ZTL* fragment was subcloned to the *Kpn* I and *Xma* I sites of the *pCsVMV-LUC-1300* vector. The *Agrobacterium* carrying either *CsVMV:ZTL-LUC* or *GUS-HA* plasmids individually, as well as *35S:GFP-SDC* or *35S:GFP* were mixed and co-infiltrated into *N. benthamiana* leaves. The LUC signal was detected with a CCD camera (LN/1300-EB/1, Princeton Instruments) after two days of infiltration. An alternative assay for degradation was agro-infiltration of *ZTL-FLAG* and *GUS-HA* as well as *35S:GFP-SDC* or *35S:GFP* into *N. benthamiana* leaves. After 3 days, the total protein was extracted, and the ZTL protein abundance

was detected by immunoblotting. To examine the degradation rate of ZTL by SDC, GFP-ZTL proteins expressed from *N. benthamiana* leaves as well as protein extracts from *Arabidopsis* wild-type Col-0 or *SDC-HA* overexpressing plants were incubated for 0, 1, 2 and 3 h. Total proteins were extracted, and the GFP and HA antibodies were used to detect the ZTL protein abundance and SDC expression respectively. For ZTL protein degradation by SDC in *Arabidopsis*, *35S:GFP-SDC* overexpression lines and Col-0 were grown on MS plates for 10 days, and the seedlings were collected at ZT0 and ZT12. Total proteins were extracted as described above, and the anti-ZTL antibodies were used to blot the ZTL protein abundance.

RESULTS

Chemically inhibiting DNA methyltransferase activity lengthened the circadian period

To examine the effect of genomic cytosine methylation on the circadian clock *in planta*, we first tested the DNA methyltransferase inhibitors 5-Aza-2'-deoxycytidine (5-Aza-dC) and Zebularine (Zeb). The two cytidine analogs could covalently bind to the active sites of DNA methyltransferases to prevent their enzyme activities (49–53). These reagents were used to treat *Arabidopsis Columbia* (Col-0) seedlings that stably harbored *CCA1:LUC*, *LNK2:LUC* or *CAB2:LUC* reporters. After being grown in a 12-h light/12-h dark photocycle for eight days, the above-indicated seedlings were transferred to constant red light conditions in the absence or presence of 5-Aza-dC or Zeb. A significant lengthening of the circadian period (~0.64 h) was observed in the 20 mg/l 5-Aza-dC treatment (24.14 ± 0.11 h) compared to the mock treatment (23.5 ± 0.03 h) as shown by the real-time bioluminescence assay (Figure 1A–C and Supplementary Figure S1A, C). An even more pronounced circadian period change (~1.32 h) was observed under 40 mg/l 5-Aza-dC (24.82 ± 0.07 h) treatment, indicating that a dose-dependent effect exists (Figure 1A–C and Supplementary Figure S1A, C). Similar to 5-Aza-dC, Zeb treatment also significantly lengthened the circadian period by about 0.7 h, as reflected by the three circadian reporters (Figure 1D–F and Supplementary Figure S1B, C, and Supplementary Table S3). To further confirm the effect of 5-Aza-dC on the circadian clock, the transcript patterns of *CCA1* and *LHY*, two core circadian components, were analyzed by a time course RT-qPCR assay. A significant phase delay of endogenous *CCA1* and *LHY* was clearly observed on the fifth day in the constant light conditions, consistent with the lengthening of the circadian period in the plants with introduced circadian reporters (Figure 1G and H), suggesting *bona fide* effects of these reagents.

As the circadian period varies among different *Arabidopsis* ecotypes due to their natural geographic origin (54), we further examined the effect of 5-Aza-dC treatment on the circadian clock in a few additional natural accessions, including *Cvi* (*Cape verde islands*), *Ws* (*Wassileskija*) and *Ler* (*Landsberg erecta*) (Supplementary Figure S1D–F). Consistent with previous findings (55,56), the *Cvi* ecotype showed a relatively shorter circadian period (21.93 ± 0.16 h) without treatment compared to *Ler* (23.65 ± 0.08 h) and *Ws*

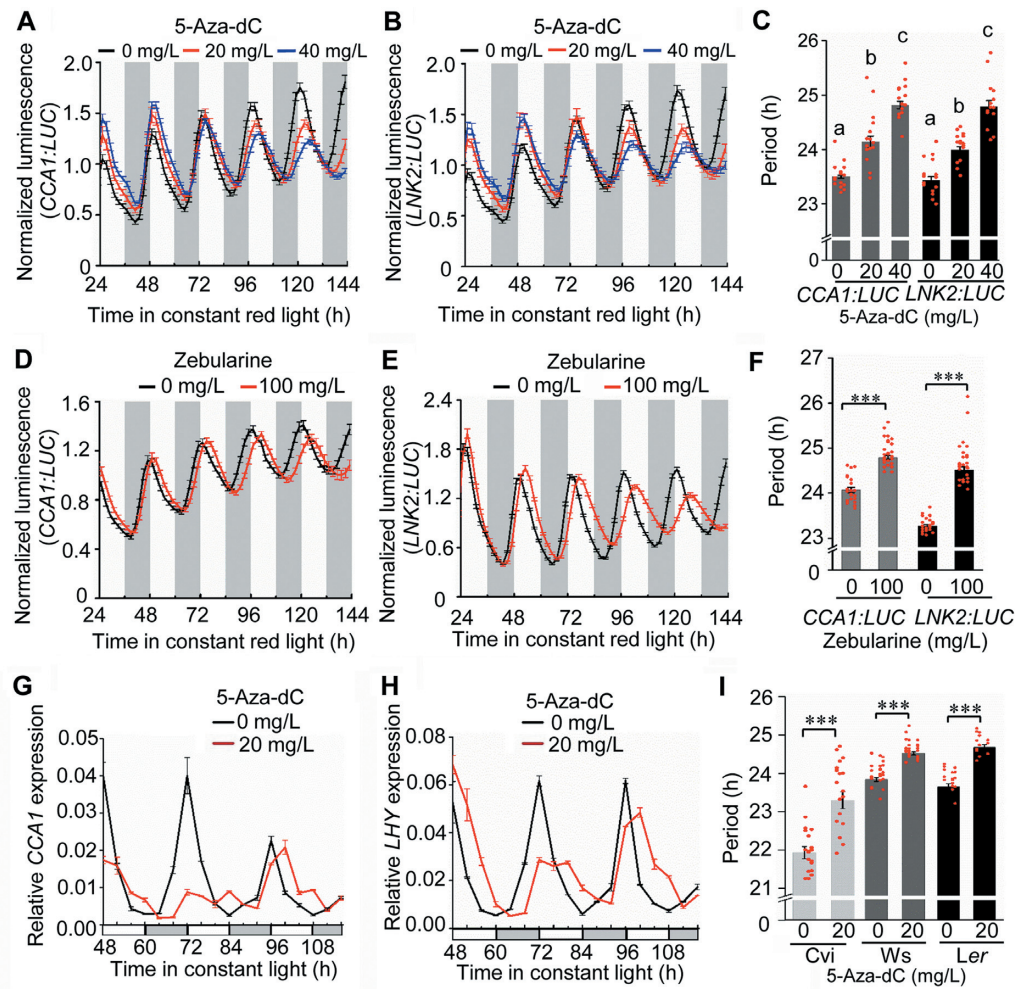


Figure 1. Chemically inhibiting DNA methyltransferases activity lengthens circadian period. (A, B) Normalized luminescence traces of *Col-0 CCA1:LUC* (A) and *Col-0 LNK2:LUC* (B) in the absence or presence of DNA methyltransferases inhibitor 5-Aza-dC (20 or 40 mg/l). The indicated *Arabidopsis* seeds harboring *CCA1:LUC* or *LNK2:LUC* reporters, were entrained in 12-h light/12-h dark at 22°C for 8 days, and were then transferred to the plates with different concentration of DNA methyltransferase inhibitors 5-Aza-dC (20 or 40 mg/l) for image acquisition under constant red light conditions at 22°C. For *Col-0* with *CCA1:LUC* reporter, 0 mg/l 5-Aza-dC, n = 19, 20 mg/l 5-Aza-dC, n = 18, 40 mg/l 5-Aza-dC, n = 18. For *Col-0* with *LNK2:LUC* reporter, 0 mg/l 5-Aza-dC, n = 18, 20 mg/l 5-Aza-dC, n = 18, 40 mg/l 5-Aza-dC, n = 15. White and gray regions indicate subjective day and night respectively. (C) The estimated circadian period in (A) and (B) calculated by Fast Fourier Transform Nonlinear Least Squares (thereafter as FFT-NLLS) analysis. Letters (a, b, c) indicate significant differences by one-way ANOVA followed by the Fisher's LSD test. (D, E) Normalized luminescence traces of *CCA1:LUC* (D) and *LNK2:LUC* (E) in the absence or presence of Zebularine. The indicated *Arabidopsis* seeds harboring *CCA1:LUC* or *LNK2:LUC* reporters, were grown in 12-h light/12-h dark at 22°C for 8 days, and were then transferred to the plates with different concentration of DNA methyltransferase inhibitors Zebularine (100 mg/l) for image acquisition under constant red light conditions at 22°C. For *Col-0* with *CCA1:LUC* reporter, 0 mg/l Zeb, n = 23, 100 mg/l Zeb, n = 29; for *Col-0* with *LNK2:LUC* reporter, 0 mg/l Zeb, n = 25, 100 mg/l Zeb, n = 26. (F) The estimated circadian period in (D) and (E) calculated by FFT-NLLS analysis. (G, H) Temporal transcriptional patterns of *CCA1* (G) and *LHY* (H) under the constant light conditions with the treatment of 5-Aza-dC. *Arabidopsis* *Col-0* grown in 12 h light/12 h dark for 8 days, and then were transferred to constant light conditions in the absence or presence of 20 mg/l 5-Aza-dC. Samples were harvested from LL48 h to LL116 h with 4-h intervals as noted. From (A) to (F) at least three independent experiments were carried out and achieved similar results. (I) Circadian phenotype of the tested *Arabidopsis* ecotypes treated by 5-Aza-dC. *Arabidopsis* ecotype *Cvi*, *Ler* and *Ws* with *CCA1:LUC* reporter were examined in the absence or presence of 20 mg/l 5-Aza-dC. In (C), (F) and (I), For *Cvi* with *CCA1:LUC* reporter, 0 mg/l 5-Aza-dC, n = 19, 20 mg/l 5-Aza-dC, n = 18; for *Ws* with *CCA1:LUC* reporter, 0 mg/l 5-Aza-dC, n = 28, 20 mg/l 5-Aza-dC, n = 28, for *Ler* with *CCA1:LUC* reporter, 0 mg/l 5-Aza-dC, n = 17, 20 mg/l 5-Aza-dC, n = 16; data represent mean ± s.e.m. (**P < 0.001, Student's t-test).

(23.83 ± 0.05 h) (Figure 1I). Nevertheless, all examined ecotypes displayed a significantly lengthened circadian period with a range of 0.68–1.37 h after 20 mg/l 5-Aza-dC treatment compared to their respective mock-treated controls (Figure 1I and Supplementary Table S3) (*Cvi* 23.30 ± 0.22 h; *Ler* 24.68 ± 0.07 h, and *Ws* 24.51 ± 0.04 h). Taken together, we conclude that pharmacological inhibition of DNA methyltransferase activity could significantly

lengthen the circadian period in the tested *Arabidopsis* accessions.

Genetically disrupting DNA methyltransferases altered circadian pace

In plants, the 5-methylcytosine in a distinct cytosine context is maintained by different DNA methyltransferases. It is well known that CG methylation is maintained by

MET1 and CMT3 is the main CHG methyltransferase, while mCHH (where H = A, T or C) is generally maintained by DRM2 and CMT2 (26,34). To examine which cytosine contexts are involved in the regulation of the circadian clock, we introgressed a series of DNA methyltransferase mutants into wild type plants that harbored the *CCA1:LUC* reporter and measured their circadian phenotypes. The homozygous *met1-3* mutant, presumably with the CG methylation nearly lost in the whole genome and associated with lower fertility (33,57), displayed a significant lengthening of the circadian period of about 1 h (Figure 2A–C and Supplementary Table S4) (Col-0 23.14 ± 0.04 h, *met1-3* 24.10 ± 0.06 h; $P < 0.001$, *t*-test), suggesting that CG methylation is involved in the regulation of the circadian clock. To determine whether the modulation of the circadian period depends on light quality, we further examined the circadian phenotypes of the above mutants under continuous monochromatic blue light. A significantly lengthened circadian period was similarly observed under continuous blue light conditions in *met1-3* mutants (Figure 2D–F and Supplementary Table S4) (Col-0 23.35 ± 0.07 h, *met1-3* 24.41 ± 0.04 h; $P < 0.001$, *t*-test), indicating that the effect of CG hypomethylation on the clock tempo is likely independent of light quality. Interestingly, we found that the *met1-3* mutant exhibited a more pronounced decrease in rhythmicity under red light than under blue light (Supplementary Figure S2A and B).

Next, we examined the effect of non-CG (CHG and CHH) methylation on the circadian clock. Although the *cmt2-3*, *cmt2-3 cmt3-11t*, *drm1-2 drm2-2* and *drm1-2 drm2-2 cmt2-3* (*ddc2*) mutants exhibited similar circadian periods to the control plants (Supplementary Figure S3A–D), the *drm1-2 drm2-2 cmt3-11t* (*ddc3*) triple mutant, in which CHG methylation was dramatically reduced (58), displayed a lengthened circadian period by ~0.9 h as measured with the *CCA1:LUC* reporter and approximately 0.7 h with the *LNK2:LUC* reporter (Figure 3A–C and Supplementary Figure S3E and F) (Col-0 23.08 ± 0.06 h and *ddc3* 23.99 ± 0.05 h for *CCA1:LUC*; Col-0 23.21 ± 0.04 h and *ddc3* 23.98 ± 0.05 h for *LNK2:LUC*; $P < 0.001$, *t*-test). Since *DRM1*, *DRM2*, *CMT2* and *CMT3* are collectively responsible for non-CG methylation, non-CG methylation in the *Arabidopsis* genome was nearly eliminated in the *drm1-2 drm2-2 cmt2-3 cmt3-11t* (*ddc2c3*) quadruple mutant (59). Notably, the *ddc2c3* quadruple mutant exhibited a significantly lengthened circadian period by about 0.8 h (*ddc2c3* 24.08 ± 0.05 h), with a slightly increasing trend (though not statistically significant) relative to that of the *ddc3* triple mutant (23.99 ± 0.05 h) (Figure 3A–C). A significantly lengthened circadian period (by about 0.8 h) was also observed under continuous monochromatic blue light (Figure 3D–F and Supplementary Table S5) (Col-0 23.23 ± 0.03 h; *ddc2c3* 24.02 ± 0.07 h). Together, these data suggested that the non-CG methylation level was also important for the modulation of the circadian clock, in which CHG methylation plays a major role. Collectively, our data clearly demonstrated that DNA cytosine methylation is a novel cellular parameter involved in modulating the circadian clock in *Arabidopsis*, irrespective of light quality.

Abnormal hypocotyl growth is considered as a hallmark of an altered circadian clock (60,61). Thus, the hypocotyl

length of the *ddc3* mutant grown under 12-h light/12-h dark was examined. Indeed, we found that the *ddc3* and *ddc2c3* mutants displayed a significantly shorter hypocotyl phenotype compared to that of wild type plants (Figure 3G and H, Supplementary Table S6), implying that non-CG DNA methylation-mediated circadian period alteration may confer changes in clock-controlled outputs such as hypocotyl growth. The mechanistic connection between the oscillator and hypocotyl growth is still unknown.

***SDC* is a candidate target to mediate the DNA hypomethylation-controlled circadian clock**

The enrichment of the DNA cytosine methylation within the promoter region is usually correlated with the degree of gene transcriptional repression. Hence, we reasoned that the 5mC level might directly affect the transcription of certain core clock components, which would subsequently affect the circadian period. We were thus led to investigate the transcript abundance of candidate clock genes at the whole-genome level. RNA-sequencing was used to identify differentially expressed clock genes after 5-Aza-dC treatment under 12-h light/12-h dark conditions. Surprisingly, among the 346 and 626 up-regulated genes at ZT1 and ZT13, respectively (Supplementary Dataset S1), none of the known clock genes had a cut-off of over 1.5 (log₂ fold change, $P < 0.05$) (Supplementary Figure S4A and B). Furthermore, for the *ddc2c3* mutant under constant white light conditions, only 163 and 105 up-regulated genes were identified at LL24 (subjective dawn) and LL36 (subjective dusk), respectively, and again no clock genes were identified in these groups (Figure 4A, B and Supplementary Dataset S2). Moreover, neither were clock genes present in the up-regulated gene list from the *met1-3* mutant from a public database (62). Nonetheless, our current transcriptomic analysis suggested that DNA hypomethylation control of circadian rhythms may not act through directly releasing the transcriptional inhibition of known clock components, but instead likely acts through other unknown factors.

To identify the novel potential factors that mediate DNA hypomethylation modulation of the circadian clock, we examined the co-regulated genes between 5-Aza-dC-treated wild-type and the DNA methyltransferase mutants, as both exhibited a lengthened circadian period. In total, seven common genes were found among the lists of up-regulated genes (Figure 4C and D), and their CG or non-CG methylation levels were indeed reduced in *met1* or *ddc3* mutants (Figure 4E and Supplementary Figure S5A, B), while no co-occurring down-regulated genes were found (Supplementary Figure S6A). Furthermore, we compared these seven common up-regulated genes with up-regulated genes in the *ddc3* mutant and found that the transcript levels of AT3G30720 (*Qua-Quine Starch, QQS*), AT2G17690 (*SDC*) and AT2G34655 were elevated in both *met1* and *ddc3* mutants (Supplementary Figure S6B). Among these, AT2G34655 encodes a hypothetical protein composed of only 22 amino acids, while the transcript of *QQS* encodes a protein of 59 amino acids that was shown to modulate starch biosynthesis (63). Interestingly, *SDC*, which was previously identified as an imprinted gene encoding an F-box containing protein (43), had the highest fold change among

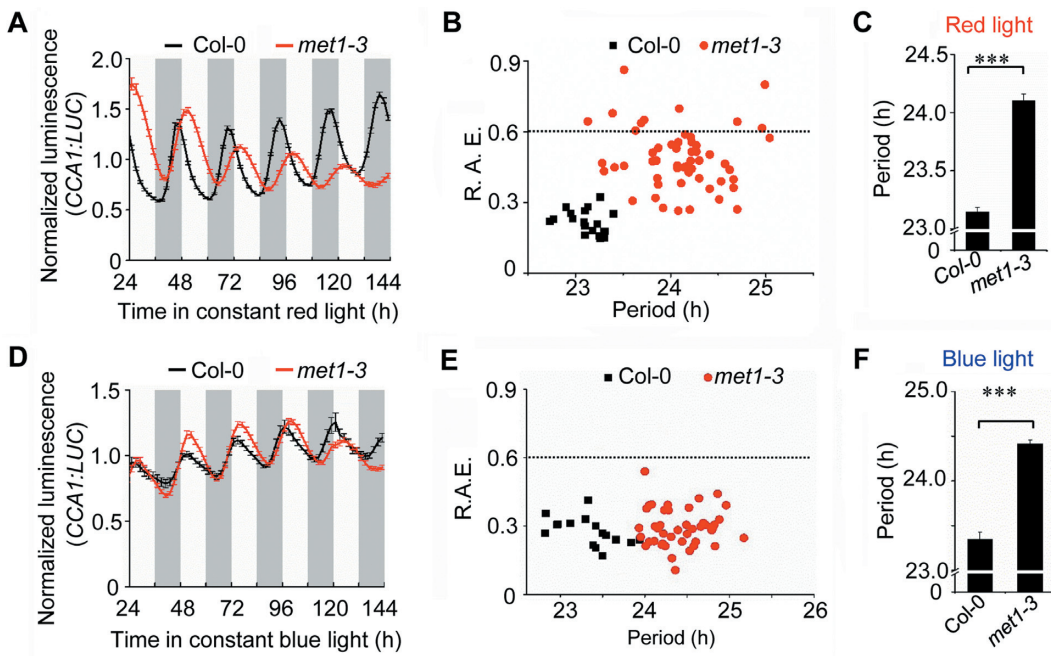


Figure 2. Loss of function of CG DNA methyltransferase *MET1* elongates circadian period. (A, D) Normalized bioluminescence traces of *CCAI:LUC* in Col-0 and *met1-3* mutant. The indicated *Arabidopsis* plants grown in 12-h light/12-h dark for 8 days, and then were transferred to constant red (A), or blue light conditions (D) for image acquisition with 2-h intervals. Under red light conditions, Col-0, $n = 42$, *met1-3*, $n = 55$ (A–C); under blue light conditions, Col-0, $n = 16$; *met1-3*, $n = 43$ (D–F). White and gray regions indicate subjective day and night respectively. (B, E) Scatter plot showing relative amplitude error (R.A.E.) versus circadian period of Col-0 and *met1-3* mutant under continuous red (B) or blue (E) light conditions. (C, F) The estimated circadian period in Col-0 and *met1-3* mutant by FFT-NLLS analysis. Data represent mean \pm s.e.m. (**P < 0.001, Student's t-test).

the seven overlapped genes (Figure 4A, B and D). Importantly, the *SDC* promoter contains high levels of cytosine DNA methylation (64), including both CG and non-CG contexts in Col-0, but these levels were markedly diminished or almost eliminated in both the *met1* and *ddc3* triple mutants and were negatively correlated with higher raw reads of mRNA (Figure 4E). Previously, the expression of *SDC* was shown to be activated in endosperm after fertilization or by external heat stress (65,66). To examine whether *SDC* is a potential causal factor for mediating DNA methylation-controlled circadian rhythms, the temporal expression level of *SDC* was examined by time-course RT-qPCR in the *ddc2c3*, *met1* mutant and Col-0. We found that *SDC* displayed extremely low expression in Col-0, but strong and rhythmic expression in the *ddc2c3* and *met1-3* mutants (Figure 4F and Supplementary Figure S7), suggesting that it may be involved in the regulation of the circadian clock. Together, these data suggested that *SDC* may be a candidate target involved in mediating the DNA methylation-modulated circadian clock.

SDC is required for the DNA hypomethylation-controlled circadian clock

To detect the role of *SDC* in the circadian clock, we initially generated *SDC*-overexpressing lines in Col-0 *CCAI:LUC* background. Two individual homozygous *CsVMV:SDC-HA* overexpression lines were obtained. Both lines contained dramatically higher *SDC* transcript levels (Figure 5A), and *SDC* protein abundance was examined by immunoblotting (Figure 5B). Notably, these overexpression

lines displayed a longer circadian period of about 0.5 h under either constant red (Figure 5C and D, Supplementary Table S7) (*CsVMV:SDC-HA* L1 23.34 ± 0.06 h and L2 23.38 ± 0.06 h, Col-0 22.82 ± 0.04 h) or blue light conditions (Supplementary Figure S8A–C and Supplementary Table S8; *CsVMV:SDC-HA* L1 24.47 ± 0.07 h and L2 24.40 ± 0.06 h, Col-0 23.54 ± 0.06 h) compared to the control. Similarly, two individual homozygous 35S:*GFP-SDC* overexpression lines also exhibited longer circadian periods by about 0.9 h under constant blue light conditions (Supplementary Figure S8D–H), suggesting that *SDC* is involved in the modulation of the circadian period. To genetically examine whether DNA methylation modulated the circadian period through *SDC*, due to the lower fertility of the *met1-3* mutant, we crossed the *ddc2c3* mutant with the *sdc* mutant. As shown in Figure 5E and F, under constant red light conditions, (Col-0 23.20 ± 0.05 h, *ddc2c3* 23.93 ± 0.08 h, *sdc* 23.25 ± 0.06 h, *ddc2c3 sdc* 23.26 ± 0.06 h) (Supplementary Table S7) and constant blue light conditions (Supplementary Figure S9A, B) (Col-0 23.58 ± 0.03 h, *ddc2c3* 24.42 ± 0.03 h, *sdc* 23.73 ± 0.07 h, *ddc2c3 sdc* 23.82 ± 0.04 h) (Supplementary Table S9), the lengthened circadian period of *ddc2c3* could be completely reverted by the *SDC* null mutation, indicating that *SDC* was required for a non-CG DNA hypomethylation-regulated circadian period. We also measured the circadian period of the *sdc* mutant in the presence of the DNA methylase inhibitor 5-Aza-dC. The period was significantly elongated after the inhibitor treatment in the *sdc* mutant, but the extent was significantly compromised relative to the corresponding period change in Col-0 plants (Supplementary Figure S10A–D), indicating that *SDC* par-

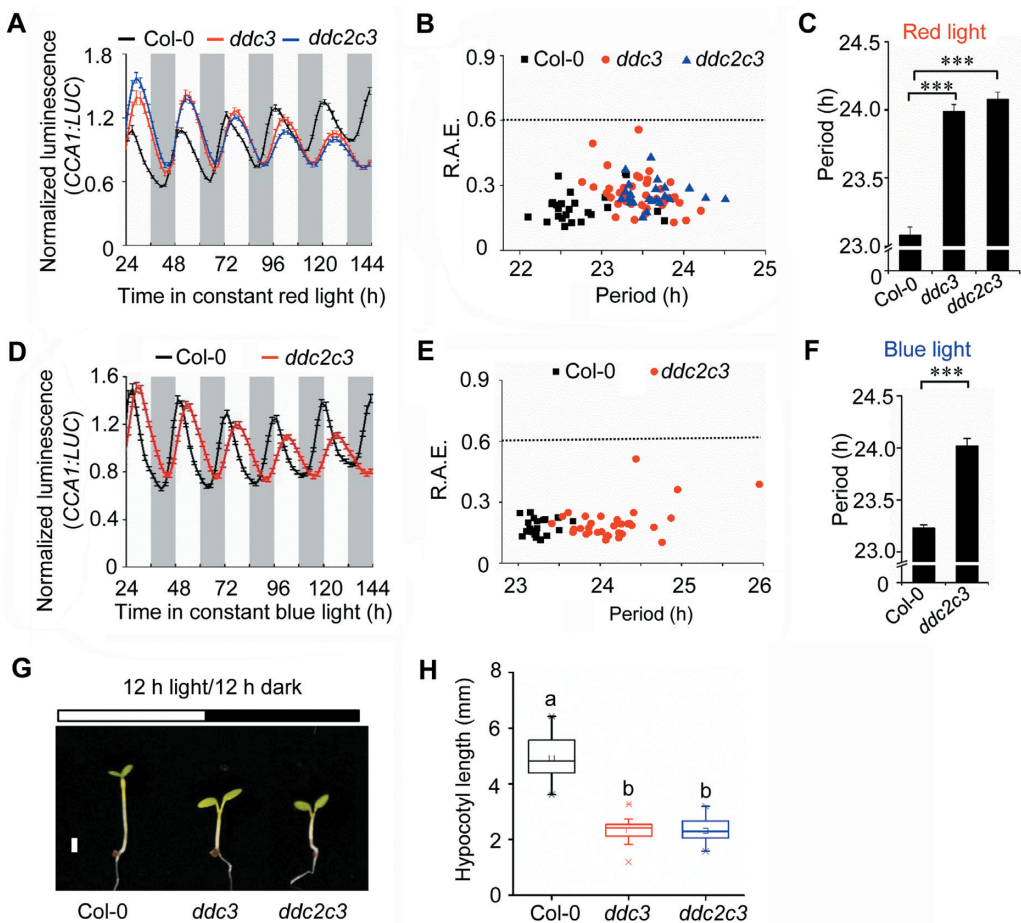


Figure 3. Deficiency of non-CG DNA methyltransferases affects circadian clock and photoperiodic hypocotyl growth. **(A)** Normalized bioluminescence traces of *CCA1:LUC* in *drm1-2 drm2-2 cmt3-11t* (here abbreviated as *ddc3*) triple mutant, *drm1-2 drm2-2 cmt2-3 cmt3-11t* (here abbreviated as *ddc2c3*) quadruple mutant and Col-0 under continuous red light conditions. The indicated *Arabidopsis* plants entrained in 12-h light/12-h dark for 8 days, and then were transferred to constant red light conditions for image acquisition with 2-h intervals. Col-0, $n = 25$; *ddc3* mutant, $n = 38$; *ddc2c3* mutant, $n = 24$. **(B)** Scatter plot showing the estimated circadian period versus R.A.E. of Col-0, *ddc3* and *ddc2c3* mutants under continuous red light condition. **(C)** Statistic analysis of the circadian period in Col-0, *ddc3* and *ddc2c3* mutants. Col-0, $n = 25$, *ddc3*, $n = 38$, *ddc2c3*, $n = 24$. Data represent mean \pm s.e.m. (** $P < 0.001$, Student's *t*-test). **(D)** Normalized bioluminescence traces of *CCA1:LUC* in *ddc2c3* quadruple mutant and Col-0 under continuous blue light condition. The indicated *Arabidopsis* plants entrained in 12 h light/12 h dark for 8 days, and then were transferred to constant blue light conditions for image acquisition with 2-h intervals. Col-0, $n = 21$; *ddc2c3* mutant $n = 34$. **(E)** Scatter plot showing the estimation of circadian period versus R.A.E. in Col-0 and *ddc2c3* mutant under continuous blue light conditions. **(F)** Statistic analysis of the circadian period in Col-0 and *ddc2c3* mutants. Data represent mean \pm s.e.m. (** $P < 0.001$, Student's *t*-test). **(G)** Hypocotyl phenotype and length measurements of Col-0, *ddc3* and *ddc2c3*. Seeds were sown on MS plates and stratified at 4°C for 3 days, and then were transferred to 12 h light/12 h dark conditions for 5 days at 22°C. Col-0, $n = 32$; *ddc3* mutant, $n = 32$; *ddc2c3* mutant, $n = 27$. The hypocotyl length was measured with ImageJ software. Scale bar, 1 mm. Letters (a, b) indicate significant differences by one-way ANOVA followed by the Fisher's LSD test.

tially mediates the effect of 5-Aza-dC on circadian rhythms, in contrast to the *sdc* mutant fully reverting the lengthened period in the *ddc2c3* mutant. This could be due to 5-Aza-dC working as a cytidine analog, thereby affecting multiple cytidine-involved processes such as genome stability (67) in addition to DNA methylation.

Moreover, the shorter hypocotyl phenotype of the *ddc2c3* mutant grown under different photoperiod conditions (12-h light/12-h dark, 8-h light/16-h dark and 16-h light/8-h dark) was also markedly rescued by the loss-of-function of *SDC* (Figure 5G and H, Supplementary Figure S11A–D, and Supplementary Table S10). In addition, plants overexpressing *SDC* also exhibited shortened hypocotyl length, resembling the *ddc2c3* quadruple mutant (Figure 5G and H, Supplementary Figure S11A–D, and Supplementary Table

S10). Together, we conclude that *SDC* is a novel circadian regulator that mediates DNA methylation-controlled circadian period and hypocotyl length.

SDC directly interacts with the ZTL protein to affect its stability

SDC encodes an F-box protein, a critical subunit for substrate recognition in SCF (Skp, Cullin, F-box) type E3 ubiquitin ligase complex that catalyzes ubiquitination of target proteins for degradation. To further gain insights into the potential targets of *SDC* in circadian clock regulation, we performed a bimolecular fluorescence complementation (BiFC) assay in *N. benthamiana* leaves to screen for interacting proteins from about 20 functional verified

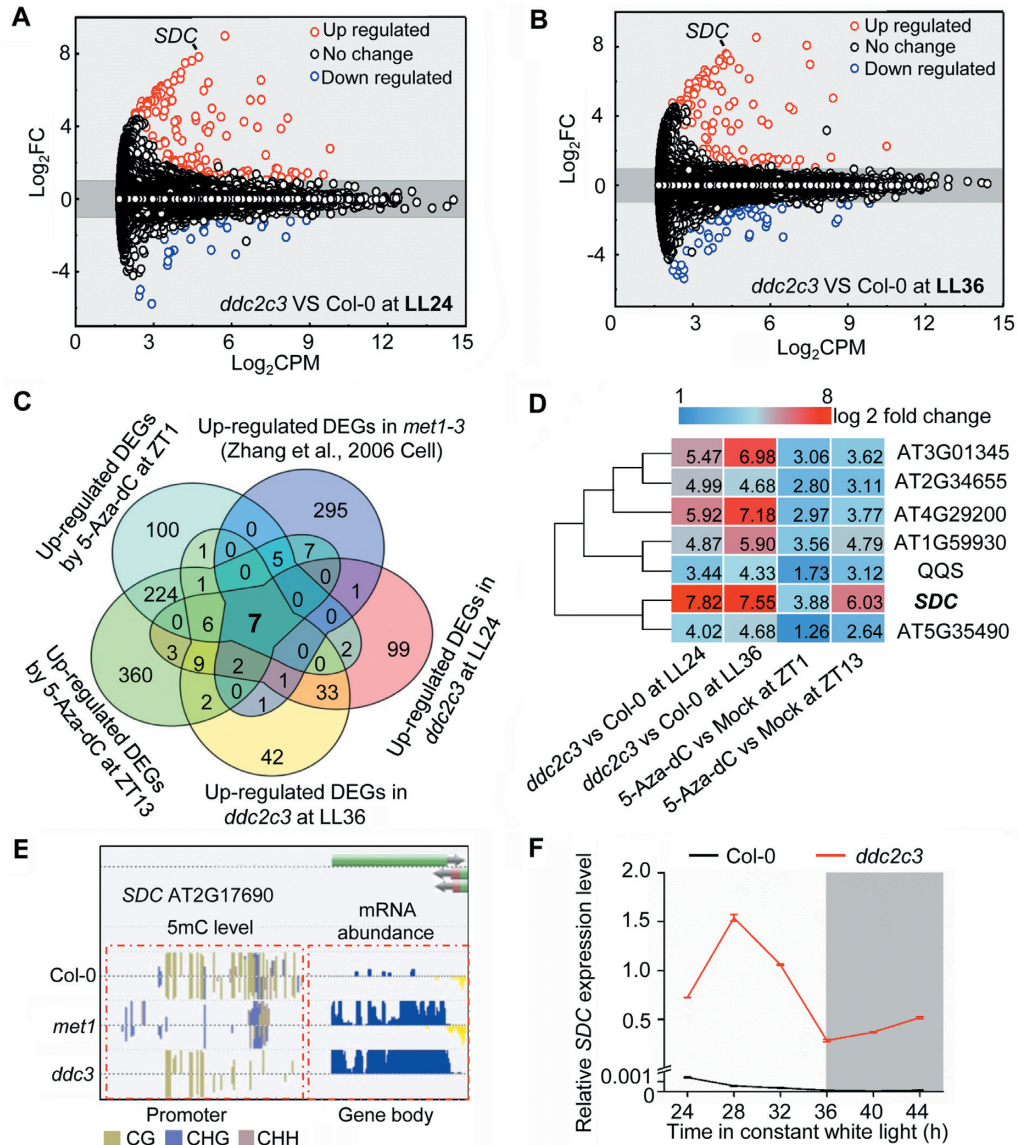


Figure 4. *SDC* is a candidate target to mediate DNA hypomethylation lengthened circadian period. (A, B) Volcano plot showing the differentially expressed genes (DEGs) in *ddc2c3* at LL24 h (A) or LL36 h (B). The x-axis indicates $\log_2\text{CPM}$ (counts per million), while the y-axis indicates $\log_2\text{FC}$ (Fold change) of the different expression genes about *ddc2c3* versus Col-0 at LL24 h or LL36 h. The shade area indicates the value of $\log_2\text{FC}$ between -1 and 1. (C) Venn diagram shows the overlapped gene number among the up-regulated genes in *met1* mutant (62) and in *ddc2c3* mutant at LL24 h or LL36 h and in 5-Aza-dC versus Mock ZT1 h or ZT13 h respectively. (D) Cluster heat map analysis of the seven co-upregulated genes in (C). (E) 5mC level in *SDC* promoter region was reduced and its transcriptional abundance was correspondingly increased in *ddc3* and *met1* mutants. Data were extracted from the published database (64). (F) Temporal expression pattern of *SDC* in *ddc2c3* mutant and wild type Col-0 under constant white light condition.

Arabidopsis circadian core proteins. Among these proteins, BiFC analysis showed that SDC-nYFP could interact with ZTL-cYFP or FKF1-cYFP (Figure 6A, bottom panels) and cYFP tagged JMJD5, PRR5, and ELF4, but none of the other tested clock components (Supplementary Figure S12). Moreover, no fluorescence signals were observed in the negative control combinations (Figure 6A, top panels). As overexpression of *SDC* lengthened the circadian period, we reasoned that the mutation of its targets should also display a lengthened circadian period. Thus, we focused on ZTL and FKF1, but not JMJD5, PRR5 or ELF4, as their null mutations resulted in significantly longer circadian periods (46,68,69). To validate whether SDC directly inter-

acts with ZTL or FKF1, we next carried out Glutathione S-transferase (GST) pull-down assays. Immunoblot analysis showed that the GST-fused SDC proteins bound to both ZTL-FLAG and FKF1-HA proteins that were expressed from *N. benthamiana* leaves, whereas GST alone did not (Figure 6B and Supplementary Figure S13A), suggesting that SDC physically interacts with ZTL and FKF1 *in vitro*. To further substantiate their interaction *in vivo*, we conducted a co-immunoprecipitation (Co-IP) assay by co-expressing GFP-SDC and ZTL-FLAG or FKF1-HA in leaves of *N. benthamiana* using GFP Trap beads. Consistently, both ZTL-FLAG and FKF1-HA proteins could be specifically detected in the immunoprecipitated complex by

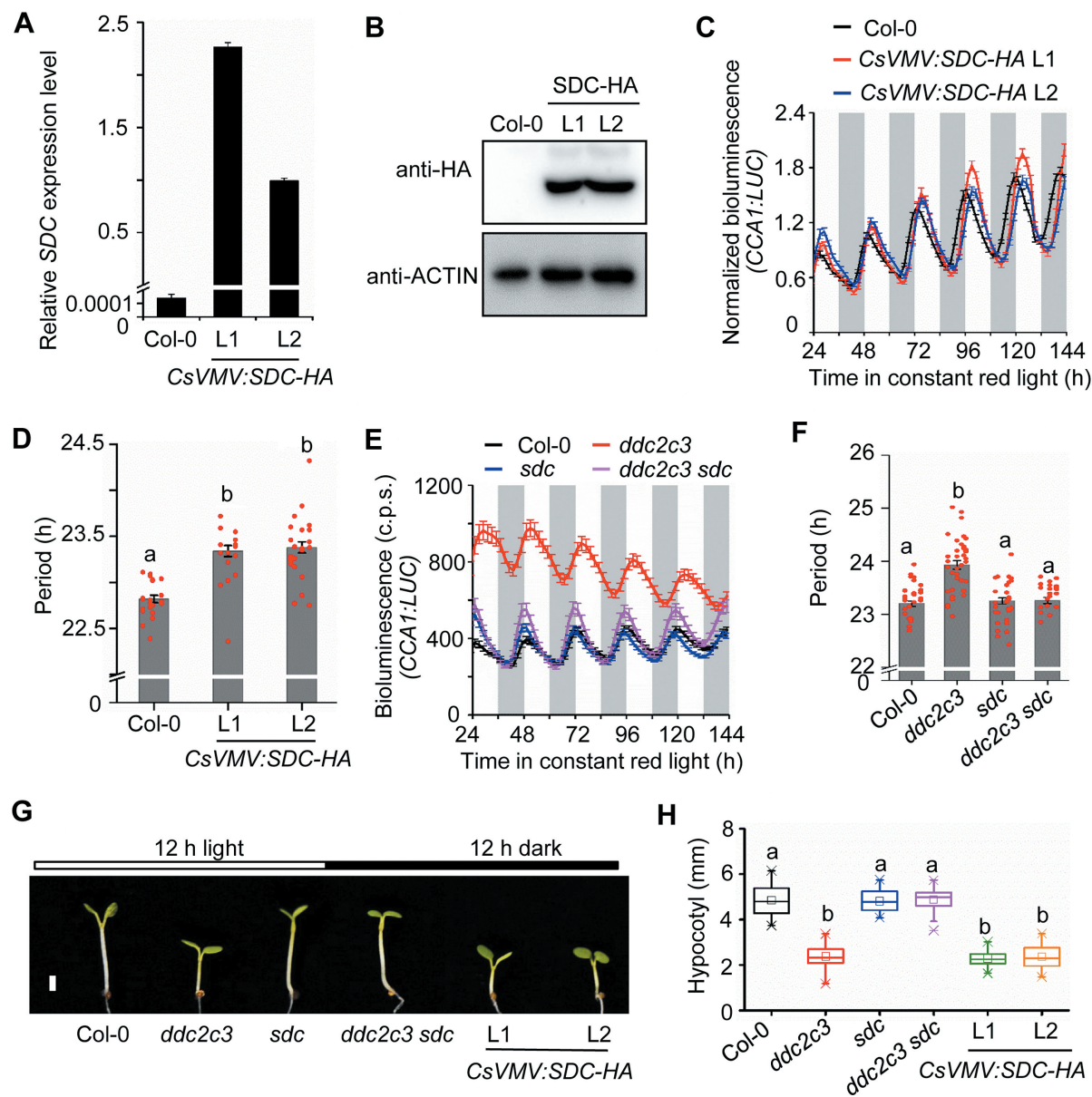


Figure 5. *SDC* is genetically required for non-CG DNA methylation-regulated circadian clock and photoperiodic hypocotyl growth. (A) Transcript level of *SDC* in two individual *CsVMV:SDC-HA* overexpressing lines and wild type Col-0 control. The geometric mean of *ACTIN2* and *TUB4* was used for normalization. (B) Immunoblot detection of *SDC-HA* protein in *CsVMV:SDC-HA* overexpressing line seedlings. ACTIN antibody was taken as loading control. (C, D) Normalized *CCA1:LUC* rhythm traces and circadian period in *CsVMV:SDC-HA* overexpressing lines. The indicated *Arabidopsis* plants grown in 12-h light/12-h dark for 8 days, and then were transferred to constant red light conditions for image acquisition with 2-h intervals. Col-0, $n = 22$; *CsVMV:SDC-HA*, line 1, $n = 15$; line 2, $n = 24$. Letters (a, b) indicate significant differences, by one-way ANOVA followed by the Fisher's LSD test. (E, F) Raw *CCA1:LUC* traces and circadian period in Col-0, *ddc2c3*, *sdc* and *ddc2c3 sdc* seedlings. The indicated *Arabidopsis* plants grown in 12-h light/12-h dark for 8 days, and then were transferred to constant red light conditions for image acquisition with 2-h intervals. Col-0, $n = 31$; *ddc2c3* mutant, $n = 39$; *sdc* mutant, $n = 29$; *ddc2c3 sdc* mutant, $n = 23$. Letters (a, b) indicate significant differences, by one-way ANOVA. (G, H) Hypocotyl phenotype (G) and length (H) of Col-0, *ddc2c3*, *sdc*, *ddc2c3 sdc* and *CsVMV:SDC-HA* transgenic lines. Seeds were sown on plates and stratified at 4°C for 3 days. Then the plates were transferred to 12-h light/12-h dark conditions to grow for additional 5 days. Col-0, $n = 35$; *ddc2c3* mutant, $n = 70$; *sdc* mutant, $n = 59$; *ddc2c3 sdc* mutant, $n = 40$. *CsVMV:SDC-HA* line 1, $n = 52$, line 2, $n = 47$. The hypocotyl length was measured with ImageJ software. Scale bar, 1 mm. Letters (a, b) indicate significant differences, by one-way ANOVA followed by the Fisher's LSD test.

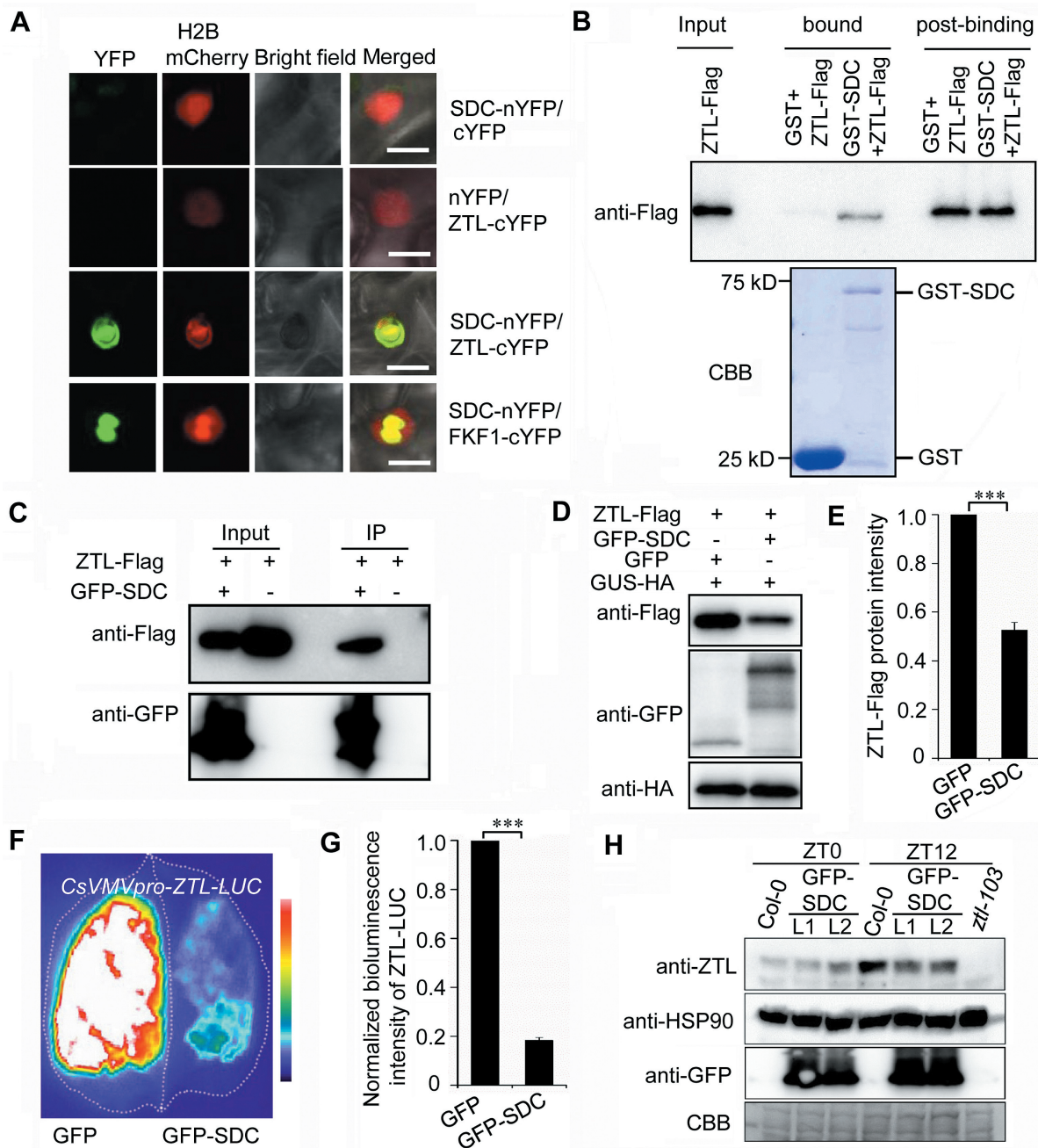


Figure 6. SDC physically interacts with ZTL to affect its protein stability. **(A)** BiFC assays showing SDC interacts with ZTL and FKF1 in *N. benthamiana* leaves. Agrobacterium strains containing SDC-nYFP/ZTL-cYFP, SDC-nYFP/FKF1-cYFP and negative controls as well as H2B-mCherry were co-infiltrated into *N. benthamiana* leaves as indicated. Scale bars, 10 µm. **(B)** GST pull-down assay between SDC and ZTL. GST or GST-SDC beads was incubated with an equal amount of *N. benthamiana* leaves expressed ZTL-FLAG extracts for 2 h. GST and its tagged proteins were analyzed by SDS-PAGE and stained by Coomassie Brilliant Blue R250 staining (CBB). Pulled-down proteins were detected by immunoblotting using FLAG antibody. **(C)** In vivo Co-IP assay of SDC with ZTL-FLAG. *N. benthamiana* leaves were agro-infiltrated with the indicated plasmid combinations. Proteins were extracted and immunoprecipitated with GFP-Trap beads. Immunoblot detection was performed using GFP or FLAG antibodies as noted. **(D, E)** Agrobacterium containing ZTL-FLAG and GFP-SDC or GFP were co-infiltrated in the *N. benthamiana* leaves for 2 days. Samples were collected and total protein was extracted. ZTL and SDC protein abundance was detected by western blot using FLAG or GFP antibody, respectively. Data represents mean ± s.e.m. ($n = 6$, *** $P < 0.001$, Student's t test). **(F, G)** ZTL abundance was reduced in the presence of SDC. *N. benthamiana* leaves were Agro-infiltrated with ZTL-LUC and GFP-SDC or GFP, 2 days later, the Luciferase signaling intensity was detected with CCD camera. The relative bioluminescence intensity of the co-infiltrated *N. benthamiana* leaves with GFP and reporter was set as 1. Data represents mean ± s.e.m. (** $P < 0.001$, Student's t test). **(H)** ZTL protein abundance in *Arabidopsis* seedlings of GFP-SDC overexpressing transgenic lines at ZT0 and ZT12. Seeds of two *Arabidopsis* GFP-SDC overexpression transgenic lines and Col-0 were sterilized and plated on MS medium with 3% sucrose. After stratification, the plates were transferred into a growth chamber with 12h light/12 h dark photoperiod at 22°C for 10 days. The seedlings were harvested at ZT0 and ZT12 for immunoblot. ZTL and GFP antibody was used for detecting ZTL and GFP-SDC, respectively. HSP90 antibody and CBB were used as the loading controls.

GFP-SDC (Figure 6C and Supplementary Figure S13B). Taken together, these results demonstrated that SDC directly interacted with ZTL and FKF1 *in vitro* and *in vivo*.

Previously, ZTL and FKF1 were characterized as F-box domain-containing blue-light photoreceptors that predominantly function in the regulation of the circadian clock and flowering time, respectively, by recognizing distinct downstream targets (18,19,70). We first investigated the rosette leaves number in the Col-0, *sdc* mutant and the *CsVMV:SDC-HA* L1 and L2 overexpression lines under 16 h light/8 h dark conditions, but there was no significant difference (Supplementary Figure S14A, B). It is possible that SDC has additional targets that may antagonize its role in flowering time regulation through FKF1 or SDC does not affect FKF1 protein abundance, which await to be further explored. As malfunction of *ZTL* significantly lengthened the circadian period, we subsequently examined whether SDC influenced the stability of ZTL. After injecting the *Agrobacterium*-containing *ZTL-FLAG* with either *GFP-SDC* or *GFP* constructs into *N. benthamiana* leaves, immunoblot detection showed that the *ZTL-FLAG* protein abundance was modestly decreased when co-expressed with *GFP-SDC*, but not *GFP* (Figure 6D and E), while the level of *ZTL* transcript was comparable in both samples (Supplementary Figure S15A), indicating that SDC may promote the degradation of ZTL. Furthermore, we co-infiltrated *ZTL-LUC* with *GFP-SDC* or *GFP* in *N. benthamiana* leaves. The bioluminescence signal of *ZTL-LUC* was significantly reduced in the presence of *GFP-SDC*, but not *GFP* (Figure 6F, G and Supplementary Figure S15B). To measure the degradation rate of ZTL by SDC, we incubated *GFP-ZTL* protein expressed from *N. benthamiana* leaves as well as protein extracts from *Arabidopsis* wild-type Col-0 or *SDC-HA* overexpressing plants for 1, 2 and 3 h. We found that the ZTL protein was gradually reduced in Col-0, and the degradation was enhanced in *SDC-HA* overexpressing lines (Supplementary Figure S16A and B). Further, the destabilization of ZTL was largely inhibited by MG132 treatment (Supplementary Figure S16C and D), suggesting SDC might affect ZTL protein turnover likely through 26S proteasome pathway. To further verify the degradation of ZTL in *Arabidopsis*, we compared the ZTL protein level in *Arabidopsis* Col-0 and two *SDC-HA* overexpression lines. Although the overexpression of *SDC* did not evidently influence the ZTL protein amount at ZT0, it significantly promoted the degradation of ZTL at ZT12 (Figure 6H), while the *ZTL* transcript levels in these materials were comparable at ZT12 (Supplementary Figure S15C). Taken together, these results demonstrate that SDC facilitated the turnover of ZTL protein *in vivo*.

ZTL acts in the same pathway with non-CG methylation to affect clock pace and hypocotyl growth

To investigate the effect of SDC on ZTL-mediated circadian period, we constructed an agro-transformation *GFP-SDC* vector in Col-0 and *ztl-3* mutant. After these materials were evaluated by RT-qPCR and western blotting (Supplementary Figure S17A and B), two independent *GFP-SDC* overexpression lines and *GFP-SDC ztl-3* transgenic lines as well as the *ztl-3* mutant were used for circadian period measure-

ment in constant red light conditions. The results demonstrated that although overexpression of *SDC* lengthened the circadian period in Col-0 wild type plants, we didn't observe further lengthening. Instead, a slight shortening circadian period in the *GFP-SDC ztl-3* transgenic lines than that in the *ztl-3* mutant was observed, indicating that ZTL is required for the effect of *SDC* overexpression on lengthening circadian period (Figure 7A and B, Supplementary Table S11 and Supplementary Figure S18A), supporting a notion that hypomethylation mediated circadian clock changes are predominantly through de-repression of SDC, which likely further promotes ZTL turnover.

To further investigate whether ZTL is a downstream target of SDC to mediate DNA hypomethylation-lengthened circadian period, a *ddc2c3 ztl* quintuple mutant was generated by genetic crossing of *ddc2c3* with *ztl-3*, a null mutant of *ZTL* (71). Homozygous F3 plants were used for examining the circadian clock phenotype. Consistent with a previous report (71), we found that *ztl-3* displayed a long circadian period but a delayed phase relative to Col-0. Importantly, there was no significant difference between the circadian period of the *ddc2c3 ztl-3* quintuple mutant (27.24 ± 0.17 h) and the *ztl-3* single mutant (27.0 ± 0.09 h). However, the circadian phase of *ddc2c3 ztl-3* quintuple mutant is similar to that of Col-0 wild type but not *ztl-3* mutant (Figure 7C–E, Supplementary Table S12, and Supplementary Figure S18B), indicating that *ZTL* likely acts in the same pathway as non-CG methyltransferases with respect to regulating the circadian period, but not the phase. However, we failed to detect the evident change of ZTL protein level in *ddc2c3* mutant at ZT0 or ZT12 (Supplementary Figure S19), which might be due to the relative lower *SDC* expression in *ddc2c3* mutant than *SDC* overexpression lines, or the sensitivity of the native ZTL antibody is not efficient to distinguish the subtle change of the ZTL protein in *ddc2c3* mutant.

Moreover, there was no additive effect between *ddc2c3* and *ztl-3* regarding photoperiodic hypocotyl growth, as demonstrated by the similar hypocotyl lengths of *ddc2c3 ztl-3* and the *ztl-3* single mutant (Figure 7F and G, Supplementary Table S13), suggesting that *ZTL* acts in the same genetic pathway as non-CG DNA hypomethylation to modulate the circadian clock.

ZTL controls the circadian period mainly through degrading the circadian core proteins TOC1 and PRR5 (18,19). TOC1 is the predominant factor in regulation of the circadian period (46). Hence, to further examine whether ZTL and its substrate protein TOC1 act in the same pathway as non-CG DNA methyltransferase, we next obtained a *ddc2c3 toc1* quintuple mutant and conducted a circadian phenotype analysis. Intriguingly, we found that the lengthened period in the *ddc2c3* mutant was significantly compromised in the *ddc2c3 toc1* quintuple mutants, with a similar circadian period as in the *toc1* mutant (Supplementary Figure S20A–C and Supplementary Table S14) (Col-0 23.08 ± 0.06 h, *ddc2c3* 24.11 ± 0.08 h, *toc1-21* 20.20 ± 0.15 h, *ddc2c3 toc1-21* 19.72 ± 0.08 h), indicating that *TOC1* is a major downstream factor of *ddc2c3* as well as *ZTL*. Altogether, we propose that the lengthened circadian period in *ddc2c3* is mainly caused by DNA methylation diminution in the *SDC* promoter that leads to the aberrant high expres-

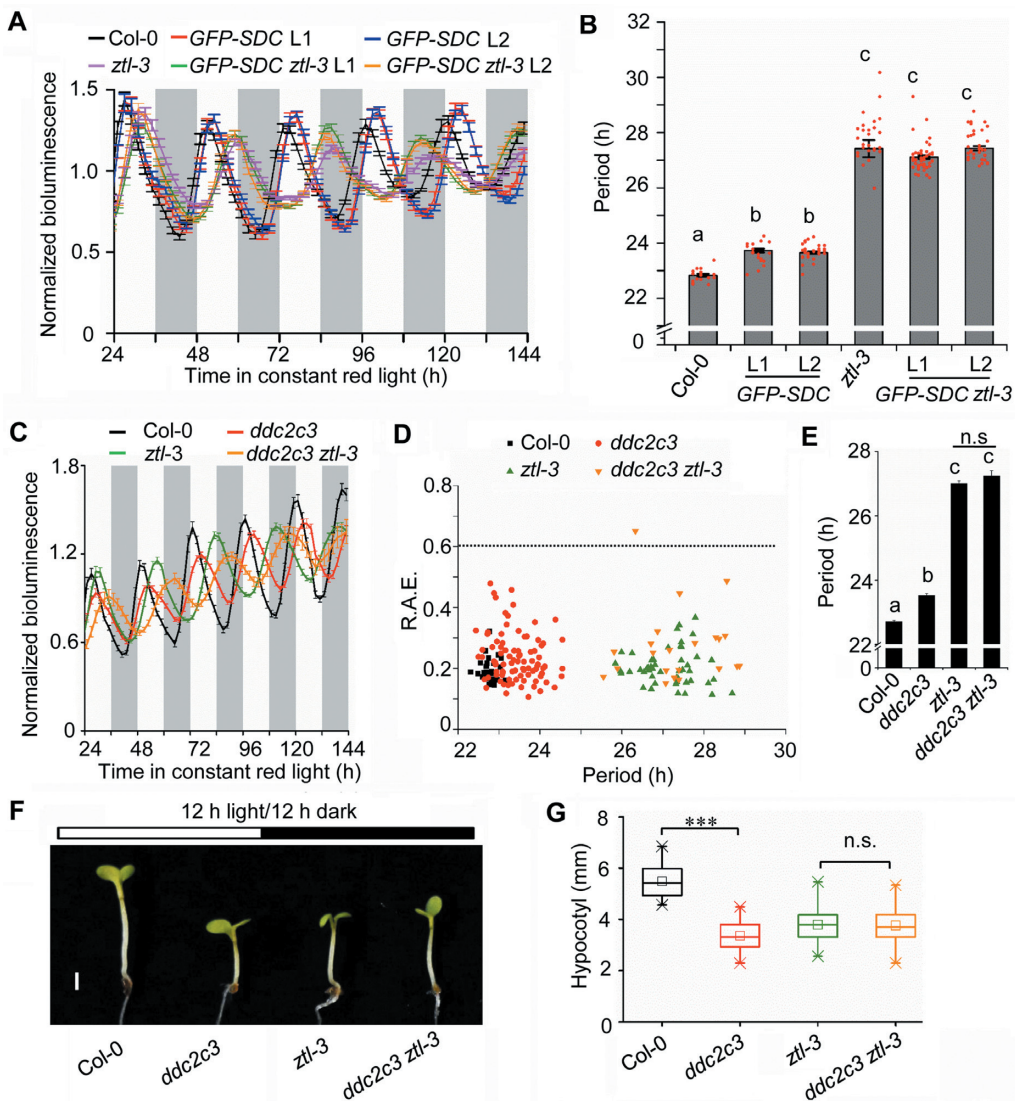


Figure 7. Non-CG methylation controlled circadian clock and hypocotyls growth is in the same genetic pathway with ZTL. (A, B) Normalized *CCAI:LUC* traces (A) and circadian period (B) of Col-0, *GFP-SDC* overexpression lines, *ztl-3* and *GFP-SDC* overexpression lines in *ztl-3* mutant. The indicated *Arabidopsis* plants grown in 12-h light/12-h dark for 8 days, and then were transferred to constant red light for image acquisition with 2-h intervals. Col-0 $n = 20$, *GFP-SDC* L1, $n = 19$, L2, $n = 33$; *ztl-3*, $n = 31$; and *GFP-SDC* *ztl-3* L1 = 47, L2 = 35. Letters (a, b, c) indicate significant differences, by one-way ANOVA followed by the Fisher's LSD test. (C–E) Normalized *CCAI:LUC* traces (C), scatter plot (D) and circadian period (E) of Col-0 ($n = 28$), *ddc2c3*, *ztl-3* and *ddc2c3 ztl-3* plants. The indicated *Arabidopsis* plants grown in 12-h light/12-h dark for 8 days, and then were transferred to constant red light conditions for image acquisition with 2-h intervals. Col-0, $n = 28$; *ddc2c3*, $n = 90$; *ztl-3*, $n = 49$; *ddc2c3 ztl-3*, $n = 22$. Letters (a, b, c) indicate significant differences, by one-way ANOVA followed by the Fisher's LSD test. (F, G) Plant phenotype (F) and hypocotyl length (G) of Col-0, *ddc2c3*, *ztl-3* and *ddc2c3 ztl-3*. Seeds were sown on plates and stratified at 4°C for 3 days and were then transferred to 12-h light/12-h dark conditions to grow for additional 5 days. Col-0, $n = 33$; *ddc2c3*, $n = 38$; *ztl-3*, $n = 44$; *ddc2c3 ztl-3*, $n = 77$. The hypocotyl length was measured with ImageJ software. Scale bar, 1 mm. Letters (a, b, c) indicate significant differences, by one-way ANOVA followed by the Fisher's LSD test.

sion level of *SDC*. Subsequently, the activated *SDC* facilitates the turnover of *ZTL*, which leads to the de-repression of *TOC1* and finally causes circadian period elongation and short hypocotyl (Figure 8).

In addition, genome-wide DNA methylation analysis of *Arabidopsis* has identified thousands of differentially methylated regions (DMRs) for local adaptation, while different ecotypes exhibit varying circadian periods due to geographical origin (72,73). Intriguingly, we found that the expression of *SDC* was significantly distinct among geographical groups, with fold differences in the hundreds

(Supplementary Figure S21) (74), implying that *SDC* likely contributes to the variation in circadian period in different ecotypes for their local adaptation. Hence, whether there are epialleles of *SDC* in mediating DNA methylation-controlled circadian pace for better regional adaptation awaits further investigation.

DISCUSSION

The circadian clock is constantly and dynamically adjusted by internal and external signals such as metabolites, hormones and photoperiod; this is termed circadian plastic-

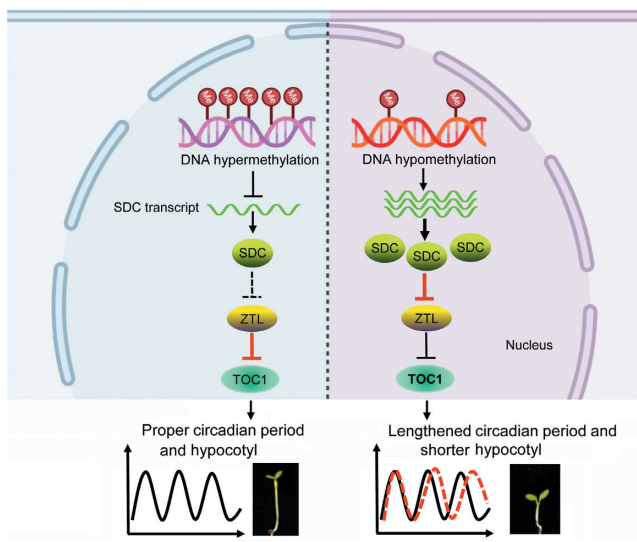


Figure 8. A proposed working model for DNA methylation controlled circadian clock. In the wild type (left panel), high levels of DNA methylation at the *SDC* promoter significantly limits its transcription, thus subsequently caused relatively higher ZTL protein level which further promotes the degradation of TOC1 protein to maintain a proper circadian period and hypocotyl length. However, when pharmacological perturbation or genetic mutation caused DNA hypomethylation at the *SDC* promoter (right panel), its transcriptional inhibition is released. The elevated SDC level likely further reduces ZTL protein stability, which caused higher TOC1 protein level and thus resulted in lengthened circadian period and shorter hypocotyl.

ity (75). However, the modification of circadian pathways through genomic methylation remains largely unexplored in many organisms. Here we showed that both CG and non-CG hypomethylation could significantly lengthen the circadian period in *Arabidopsis*. Surprisingly, RNA expression dataset analyses and promoter methylation profiles from publicly available data did not identify any of the known clock components for which their transcript levels displayed significant changes. This may be due to the limited number of time points or inconsistent light conditions among experiments. Thus, a higher resolution time course of RNA sequencing may be useful for identification of differentially expressed clock genes. Instead, we found that *SDC* was up-regulated under whole genome hypomethylated DNA conditions, while it was silenced in Col-0 under normal growth conditions due to the high level of methylation of its promoter. Consistently, overexpression of *SDC* mimicked the lengthened period found in the DNA methylation mutants (Figure 5C and D), while its mutation could dramatically revert the lengthened circadian period in the *ddc2c3* mutant (Figure 5E and F). These analyses support the notion that elevated transcript levels of *SDC* are responsible for the period effects in the methylation mutants. Intriguingly, the effect of DNA methylation on circadian phase was not rescued by the *ZTL* null mutation (Supplementary Figure S18), indicating that other downstream factors of *SDC* may be involved in DNA-methylation caused circadian phase changes. One of the candidates might be FKF1, as it also interacted with *SDC* (Supplementary Figure S13) and was shown to affect circadian parameters in concert with *ZTL*

(76). It will be interesting to test this hypothesis in the future by genetic and biochemical analyses.

Hypocotyl growth dynamics have long been thought to be due to a coincidence mechanism between the endogenous circadian clock and external day length (77). Here we found that the short hypocotyl phenotype in the *ddc2c3* mutant was also complemented by the *sdc* mutant resembling Col-0 (Figure 5G and H), suggesting that *SDC* is also crucial for DNA hypomethylation causing the short hypocotyl. This could likely attribute to the activated proteolytic cascade of SDC-ZTL-TOC1 that resulted in the higher TOC1 protein abundance, as it has been demonstrated that TOC1 can directly interact with PHYTOCHROME INTERACTING FACTORS (PIFs) to sequester their activity to promote hypocotyl elongation (78–80).

SDC is silenced in vegetative tissues but expressed in endosperm after fertilization, where it exhibited an increase by 2- to 5-fold at 2 DAP (days after pollination). However, the endosperm development in the null *sdc* mutant is normal and produced viable seeds, suggesting that *SDC* is not required for endosperm development (66,81). Nevertheless, epigenetic suppression of *SDC* seems to be essential for development, since non-CG DNA methylation mutants as well as *SDC* overexpression lines with high expression of *SDC* displayed a curled leaf phenotype during vegetative growth. Recently, it was reported that *SDC* is also activated in the *nrpd1-3 pkl-1* or *nrpe1-11 pkl-1* double mutants, which lacks both RdDM pathway and chromatin remodeling activity and exhibits a curled leaf phenotype that is strongly correlated with the up-regulation of *SDC* (82). These results suggest that in addition to non-CG DNA methylation, *PKL* acts synergistically with RdDM to repress *SDC* gene transcription. In addition, the expression of *SDC* could be induced in young developing leaves by environmental stimuli such as high temperature (65). A long-term heat stress experiment demonstrated that the *sdc* mutant showed significantly reduced biomass by approximately 30% compared to the corresponding wild type (65). These results suggest that *SDC* overexpression may contribute to the recovery of plant biomass after heat stress. However, we found no known circadian component exhibiting obvious changes in the transcriptome database of wild-type or *sdc* mutants during the recovery from heat stress entrainment (65). Hence, whether the higher temperature-induced *SDC* expression (65) could subsequently modulate the circadian clock to adapt to the unfavorable warm conditions should also be addressed. It is possible that an enhanced *SDC* level causes higher TOC1 protein abundance, which may at least inhibit the overgrowth of the petiole or hypocotyl in warm temperature (78–80), consistent with the contribution of *SDC* to the recovery of plant biomass after heat stress (65).

Ubiquitination-dependent degradation plays an important role in removal of unfolded or unnecessary proteins as well as maintaining protein stability. F-box proteins are responsible for recognizing substrates and subsequent ubiquitination by interacting with SKP1 and Cullin1 to form a functional SCF-type E3 ligase complex (83). Intriguingly, two E3 ligases synergistically regulating the same biological phenomenon has been demonstrated. For example, F-box proteins EIN3 BINDING F-BOX protein 1/2

(EBF1/2) degrade the transcription factor PIF3 in darkness to promote photomorphogenesis, while RING-finger type E3 ligase COP1 can target EBF1/2 for degradation, causing PIF3 protein accumulation (84). In our findings, the F-box domain-containing protein SDC interacted with another F-box protein ZTL and recruited ZTL for degradation. It has been shown that the ZTL-mediated circadian period is regulated through the degradation of the substrates TOC1 and PRR5 in the evening (18,19), in which TOC1 plays a more pronounced role (46,47). Our genetic evidence further showed that ZTL and its downstream target TOC1 act in the same pathway as DNA hypomethylation in its effect on clock pace and hypocotyl growth. Therefore, we propose that the proteolytic cascade of SDC-ZTL-TOC1 connected DNA methylation to the circadian clock (Figure 8). To summarize, DNA hypomethylation plays an important role in maintaining proper circadian period mainly through the reduction of SDC promoter methylation, thereby increasing its transcript level. Furthermore, elevated SDC levels subsequently facilitates the turnover of ZTL protein, which likely results in higher TOC1 protein levels, longer circadian period and a shortened hypocotyl (Figure 8). Our findings demonstrate that the DNA methylation and protein ubiquitination cooperate to maintain proper circadian protein accumulation and the internal clock rhythm.

Lastly, the role of DNA cytosine methylation in fine-tuning the circadian clock may be an evolutionarily conserved mechanism in both plants and mammals. It has been reported that circadian period change by an altered light-dark cycle requires *de novo* DNA methylation in mice (85,86). Importantly, the level of DNA methylation at some CG sites tends to increase with age in mammals (87). The improper DNA methylation could trigger abnormal clock gene expression, thus contributing to the occurrence of cancer (88). Our findings in a model plant may shed new light on the effects of DNA methylation on mammalian circadian period regulation. In closing, the role of 5mC homeostasis in assisting to tune the circadian period may optimize plant growth and development by synchronizing the internal growing phase with ever-changing environmental cues.

DATA AVAILABILITY

The RNA-seq data of *ddc2c3* mutant and 5-Aza-dC treatment was deposited to NCBI-Gene Expression Omnibus (GEO) database (GSE153510).

SUPPLEMENTARY DATA

Supplementary Data are available at NAR Online.

ACKNOWLEDGEMENTS

We are very grateful to Profs. David E. Somers and J.C. Jang from the Ohio State University for their constructive comments. We thank Dr Honggui La from Nanjing Agricultural University for *met1-3* seeds, and Dr. Xiaodong Xu from Henan University for Col-0 (*LNK2:LUC*) seeds.

FUNDING

Strategic Priority Research Program of the Chinese Academy of Sciences [XDB27030206]; National Natural Science Foundation of China [31570292]; Chinese Academy of Sciences [QYZDB-SSW-SMC011 to L.W.]. Funding for open access charge: Priority Research Program of the Chinese Academy of Sciences [XDB27030206].

Conflict of interest statement. None declared.

REFERENCES

- Malapeira,J., Khaitova,L.C. and Mas,P. (2012) Ordered changes in histone modifications at the core of the *Arabidopsis* circadian clock. *Proc. Natl. Acad. Sci. U.S.A.*, **109**, 21540–21545.
- Wang,W., Barnaby,J.Y., Tada,Y., Li,H., Tor,M., Caldelari,D., Lee,D.U., Fu,X.D. and Dong,X. (2011) Timing of plant immune responses by a central circadian regulator. *Nature*, **470**, 110–114.
- Ezer,D., Jung,J.H., Lan,H., Biswas,S., Gregoire,L., Box,M.S., Charoensawan,V., Cortijo,S., Lai,X.L., Stockle,D. et al. (2017) The evening complex coordinates environmental and endogenous signals in *Arabidopsis*. *Nat. Plants*, **3**, 17087.
- Kim,H., Kim,H.J., Vu,Q.T., Jung,S., McClung,C.R., Hong,S. and Nam,H.G. (2018) Circadian control of ORE1 by PRR9 positively regulates leaf senescence in *Arabidopsis*. *Proc. Natl. Acad. Sci. U.S.A.*, **115**, 8448–8453.
- Li,B., Wang,Y., Zhang,Y., Tian,W., Chong,K., Jang,J.-C. and Wang,L. (2019) PRR5, 7 and 9 positively modulate TOR signaling-mediated root cell proliferation by repressing TANDEM ZINC FINGER 1 in *Arabidopsis*. *Nucleic Acids Res.*, **47**, 5001–5015.
- Nakamichi,N., Kiba,T., Kamioka,M., Suzuki,T., Yamashino,T., Higashiyama,T., Sakakibara,H. and Mizuno,T. (2012) Transcriptional repressor PRR5 directly regulates clock-output pathways. *Proc. Natl. Acad. Sci. U.S.A.*, **109**, 17123–17128.
- Zhang,Y., Wang,Y., Wei,H., Li,N., Tian,W., Chong,K. and Wang,L. (2018) Circadian evening complex represses jasmonate-induced leaf senescence in *Arabidopsis*. *Mol. Plant*, **11**, 326–337.
- Dodd,A.N., Salathia,N., Hall,A., Kevei,E., Toth,R., Nagy,F., Hibberd,J.M., Millar,A.J. and Webb,A.A.R. (2005) Plant circadian clocks increase photosynthesis, growth, survival, and competitive advantage. *Science*, **309**, 630–633.
- Greenham,K. and McClung,C.R. (2015) Integrating circadian dynamics with physiological processes in plants. *Nat. Rev. Genet.*, **16**, 598–610.
- Sanchez,S.E. and Kay,S.A. (2016) The plant circadian clock: from a simple timekeeper to a complex developmental manager. *Cold Spring Harbor Perspect. Biol.*, **8**, a027748.
- Bell-Pedersen,D., Cassone,V.M., Earnest,D.J., Golden,S.S., Hardin,P.E., Thomas,T.L. and Zoran,M.J. (2005) Circadian rhythms from multiple oscillators: lessons from diverse organisms. *Nat. Rev. Genet.*, **6**, 544–556.
- Alabadi,D., Oyama,T., Yanovsky,M.J., Harmon,F.G., Mas,P. and Kay,S.A. (2001) Reciprocal regulation between TOC1 and LHY/CCA1 within the *Arabidopsis* circadian clock. *Science*, **293**, 880–883.
- Lu,S.X., Knowles,S.M., Andronis,C., Ong,M.S. and Tobin,E.M. (2009) Circadian clock associated1 and late elongated hypocotyl function synergistically in the circadian clock of *Arabidopsis*. *Plant Physiol.*, **150**, 834–843.
- Yakir,E., Hilman,D., Kron,I., Hassidim,M., Melamed-Book,N. and Green,R.M. (2009) Posttranslational regulation of circadian clock associated1 in the circadian oscillator of *Arabidopsis*. *Plant Physiol.*, **150**, 844–857.
- Nakamichi,N., Kita,M., Ito,S., Sato,E., Yamashino,T. and Mizuno,T. (2005) The *Arabidopsis* pseudo-response regulators, PRR5 and PRR7, coordinately play essential roles for circadian clock function. *Plant Cell Physiol.*, **46**, 609–619.
- Adams,S., Manfield,I., Stockley,P. and Carre,I.A. (2015) Revised morning loops of the *Arabidopsis* circadian clock based on analyses of direct regulatory interactions. *PLoS One*, **10**, e0143943.
- Nakamichi,N., Kiba,T., Henriques,R., Mizuno,T., Chua,N.H. and Sakakibara,H. (2010) Pseudo-response regulators 9, 7, and 5 are

- transcriptional repressors in the *Arabidopsis* circadian clock. *Plant Cell*, **22**, 594–605.
18. Mas,P., Kim,W.Y., Somers,D.E. and Kay,S.A. (2003) Targeted degradation of TOC1 by ZTL modulates circadian function in *Arabidopsis thaliana*. *Nature*, **426**, 567–570.
 19. Kiba,T., Henriques,R., Sakakibara,H. and Chua,N.H. (2007) Targeted degradation of pseudo-response regulator5 by an SCFZTL complex regulates clock function and photomorphogenesis in *Arabidopsis thaliana*. *Plant Cell*, **19**, 2516–2530.
 20. Hsu,P.Y. and Harmer,S.L. (2014) Wheels within wheels: the plant circadian system. *Trends Plant Sci.*, **19**, 240–249.
 21. Perales,M. and Mas,P. (2007) A functional link between rhythmic changes in chromatin structure and the *Arabidopsis* biological clock. *Plant Cell*, **19**, 2111–2123.
 22. Hung,F.Y., Chen,F.F., Li,C., Chen,C., Lai,Y.C., Chen,J.H., Cui,Y. and Wu,K. (2018) The *Arabidopsis* LDL1/2-HDA6 histone modification complex is functionally associated with CCA1/LHY in regulation of circadian clock genes. *Nucleic Acids Res.*, **46**, 10669–10681.
 23. Lee,K., Mas,P. and Seo,P.J. (2019) The EC-HDA9 complex rhythmically regulates histone acetylation at the TOC1 promoter in *Arabidopsis*. *Commun. Biol.*, **2**, 143.
 24. Wang,L., Kim,J. and Somers,D.E. (2013) Transcriptional corepressor TOPLESS complexes with pseudoreponse regulator proteins and histone deacetylases to regulate circadian transcription. *Proc. Natl. Acad. Sci. U.S.A.*, **110**, 761–766.
 25. He,X.J., Chen,T. and Zhu,J.K. (2011) Regulation and function of DNA methylation in plants and animals. *Cell Res.*, **21**, 442–465.
 26. Zhang,H., Lang,Z. and Zhu,J.K. (2018) Dynamics and function of DNA methylation in plants. *Nat. Rev. Mol. Cell Biol.*, **19**, 489–506.
 27. Tomita,T., Kurita,R. and Onishi,Y. (2017) Epigenetic regulation of the circadian clock: role of 5-aza-2'-deoxycytidine. *Biosci. Rep.*, **37**, BSR20170053.
 28. Kim,J., Samaranayake,M. and Pradhan,S. (2009) Epigenetic mechanisms in mammals. *Cell Mol. Life Sci.*, **66**, 596–612.
 29. Milagro,F.I., Gómez-Abellán,P., Campión,J., Martínez,J.A., Ordovás,J.M. and Garaulet,M. (2012) CLOCK, PER2 and BMAL1 DNA methylation: association with obesity and metabolic syndrome characteristics and monounsaturated fat intake. *Chronobiol. Int.*, **29**, 1180–1194.
 30. Taniguchi,H., Fernández,A.F., Setién,F., Ropero,S., Ballestar,E., Villanueva,A., Yamamoto,H., Imai,K., Shinomura,Y. and Esteller,M. (2009) Epigenetic inactivation of the circadian clock gene BMAL1 in hematologic malignancies. *Cancer Res.*, **69**, 8447–8454.
 31. Stroud,H., Greenberg,M.V., Feng,S., Bernatavichute,Y.V. and Jacobsen,S.E. (2013) Comprehensive analysis of silencing mutants reveals complex regulation of the *Arabidopsis* methylome. *Cell*, **152**, 352–364.
 32. Zemach,A., Kim,M.Y., Hsieh,P.H., Coleman-Derr,D., Eshed-Williams,L., Thao,K., Harmer,S.L. and Zilberman,D. (2013) The *Arabidopsis* nucleosome remodeler DDM1 allows DNA methyltransferases to access H1-containing heterochromatin. *Cell*, **153**, 193–205.
 33. Saze,H., Scheid,O.M. and Paszkowski,J. (2003) Maintenance of CpG methylation is essential for epigenetic inheritance during plant gametogenesis. *Nat. Genet.*, **34**, 65–69.
 34. Stroud,H., Do,T., Du,J., Zhong,X., Feng,S., Johnson,L., Patel,D.J. and Jacobsen,S.E. (2014) Non-CG methylation patterns shape the epigenetic landscape in *Arabidopsis*. *Nat. Struct. Mol. Biol.*, **21**, 64–72.
 35. Lindroth,A.M., Cao,X., Jackson,J.P., Zilberman,D., McCallum,C.M., Henikoff,S. and Jacobsen,S.E. (2001) Requirement of CHROMOMETHYLASE3 for maintenance of CpXpG methylation. *Science*, **292**, 2077–2080.
 36. Du,J., Johnson,L.M., Jacobsen,S.E. and Patel,D.J. (2015) DNA methylation pathways and their crosstalk with histone methylation. *Nat. Rev. Mol. Cell Biol.*, **16**, 519–532.
 37. Soppe,W.J., Jacobsen,S.E., Alonso-Blanco,C., Jackson,J.P., Kakutani,T., Koornneef,M. and Peeters,A.J. (2000) The late flowering phenotype of fwa mutants is caused by gain-of-function epigenetic alleles of a homeodomain gene. *Mol. Cell*, **6**, 791–802.
 38. He,L., Wu,W., Zinta,G., Yang,L., Wang,D., Liu,R., Zhang,H., Zheng,Z., Huang,H., Zhang,Q. et al. (2018) A naturally occurring epiallele associates with leaf senescence and local climate adaptation in *Arabidopsis* accessions. *Nat. Commun.*, **9**, 460.
 39. Cortijo,S., Wardenar,R., Colome-Tatche,M., Gilly,A., Etcheverry,M., Labadie,K., Caillieux,E., Hospital,F., Aury,J.M., Wincker,P. et al. (2014) Mapping the epigenetic basis of complex traits. *Science*, **343**, 1145–1148.
 40. Dowen,R.H., Pelizzola,M., Schmitz,R.J., Lister,R., Dowen,J.M., Nery,J.R., Dixon,J.E. and Ecker,J.R. (2012) Widespread dynamic DNA methylation in response to biotic stress. *Proc. Natl. Acad. Sci. U.S.A.*, **109**, E2183–E2191.
 41. Martin,A., Troadec,C., Boualem,A., Rajab,M., Fernandez,R., Morin,H., Pitrat,M., Dogimont,C. and Bendahmane,A. (2009) A transposon-induced epigenetic change leads to sex determination in melon. *Nature*, **461**, 1135–1138.
 42. Cao,X.F. and Jacobsen,S.E. (2002) Role of the *Arabidopsis* DRM methyltransferases in de novo DNA methylation and gene silencing. *Curr. Biol.*, **12**, 1138–1144.
 43. Henderson,I.R. and Jacobsen,S.E. (2008) Tandem repeats upstream of the *Arabidopsis* endogene SDC recruit non-CG DNA methylation and initiate siRNA spreading. *Genes Dev.*, **22**, 1597–1606.
 44. Wang,Y., He,Y., Su,C., Zentella,R., Sun,T.P. and Wang,L. (2020) Nuclear localized O-fucosyltransferase SPY facilitates PRR5 proteolysis to fine-tune the pace of *Arabidopsis* circadian clock. *Mol. Plant*, **13**, 446–458.
 45. Li,N., Zhang,Y., He,Y., Wang,Y. and Wang,L. (2020) Pseudo response regulators regulate photoperiodic hypocotyl growth by repressing PIF4/5 transcription. *Plant Physiol.*, **183**, 686–699.
 46. Fujiwara,S., Wang,L., Han,L., Suh,S.S., Salome,P.A., McClung,C.R. and Somers,D.E. (2008) Post-translational regulation of the *Arabidopsis* circadian clock through selective proteolysis and phosphorylation of pseudo-response regulator proteins. *J. Biol. Chem.*, **283**, 23073–23083.
 47. Wang,L., Fujiwara,S. and Somers,D.E. (2010) PRR5 regulates phosphorylation, nuclear import and subnuclear localization of TOC1 in the *Arabidopsis* circadian clock. *EMBO J.*, **29**, 1903–1915.
 48. Abramoff,M.D., Magalhães,P.J. and Ram,S.J.J.B.i. (2004) Image processing with ImageJ. *Biophotonics Int.*, **11**, 36–42.
 49. Christman,J.K. (2002) 5-Azacytidine and 5-aza-2'-deoxycytidine as inhibitors of DNA methylation: mechanistic studies and their implications for cancer therapy. *Oncogene*, **21**, 5483–5495.
 50. Zhou,L., Cheng,X., Connolly,B., Dickman,M., Hurd,P. and Hornby,D. (2002) Zebularine: a novel DNA methylation inhibitor that forms a covalent complex with DNA methyltransferases. *J. Mol. Biol.*, **321**, 591–599.
 51. Champion,C., Guianvarc'h,D., Senamaud-Beaufort,C., Jurkowska,R.Z., Jeltsch,A., Ponger,L., Arimondo,P.B. and Guiyesse-Peugeot,A.L. (2010) Mechanistic insights on the inhibition of c5 DNA methyltransferases by zebularine. *PLoS One*, **5**, e12388.
 52. Lang,Z., Lei,M., Wang,X., Tang,K., Miki,D., Zhang,H., Mangrauthia,S.K., Liu,W., Nie,W. and Ma,G. (2015) The methyl-CpG-binding protein MBD7 facilitates active DNA demethylation to limit DNA hyper-methylation and transcriptional gene silencing. *Mol. Cell*, **57**, 971–983.
 53. Griffin,P.T., Niederhuth,C.E. and Schmitz,R.J. (2016) A comparative analysis of 5-azacytidine- and zebularine-induced DNA demethylation. *G3 (Bethesda)*, **6**, 2773–2780.
 54. Edwards,K.D., Lynn,J.R., Gyula,P., Nagy,F. and Millar,A.J. (2005) Natural allelic variation in the temperature-compensation mechanisms of the *Arabidopsis thaliana* circadian clock. *Genetics*, **170**, 387–400.
 55. Swarup,K., Alonso-Blanco,C., Lynn,J.R., Michaels,S.D., Amasino,R.M., Koornneef,M. and Millar,A.J. (1999) Natural allelic variation identifies new genes in the *Arabidopsis* circadian system. *Plant J.*, **20**, 67–77.
 56. Kim,T.S., Wang,L., Kim,Y.J. and Somers,D.E. (2020) Compensatory mutations in GI and ZTL may modulate temperature compensation in the circadian clock. *Plant Physiol.*, **182**, 1130–1141.
 57. Mathieu,O., Reinders,J., Čaikovski,M., Smathajitt,C. and Paszkowski,J. (2007) Transgenerational stability of the *Arabidopsis* epigenome is coordinated by CG methylation. *Cell*, **130**, 851–862.
 58. Cokus,S.J., Feng,S., Zhang,X., Chen,Z., Merriman,B., Haudenschild,C.D., Pradhan,S., Nelson,S.F., Pellegrini,M. and Jacobsen,S.E. (2008) Shotgun bisulphite sequencing of the *Arabidopsis* genome reveals DNA methylation patterning. *Nature*, **452**, 215–219.

59. Stroud,H., Do,T., Du,J., Zhong,X., Feng,S., Johnson,L., Patel,D.J. and Jacobsen,S.E. (2014) Non-CG methylation patterns shape the epigenetic landscape in *Arabidopsis*. *Nat. Struct. Mol. Biol.*, **21**, 64–72.
60. Dowson-Day,M.J. and Millar,A.J. (1999) Circadian dysfunction causes aberrant hypocotyl elongation patterns in *Arabidopsis*. *Plant J.*, **17**, 63–71.
61. Nagel,D.H. and Kay,S.A. (2012) Complexity in the wiring and regulation of plant circadian networks. *Curr. Biol.*, **22**, R648–R657.
62. Zhang,X., Yazaki,J., Sundaresan,A., Cokus,S., Chan,S.W., Chen,H., Henderson,I.R., Shinn,P., Pellegrini,M., Jacobsen,S.E. *et al.* (2006) Genome-wide high-resolution mapping and functional analysis of DNA methylation in *Arabidopsis*. *Cell*, **126**, 1189–1201.
63. Li,L., Foster,C.M., Gan,Q.L., Nettleton,D., James,M.G., Myers,A.M. and Wurtele,E.S. (2009) Identification of the novel protein QQS as a component of the starch metabolic network in *Arabidopsis* leaves. *Plant J.*, **58**, 485–498.
64. Lister,R., O’Malley,R.C., Tonti-Filippini,J., Gregory,B.D., Berry,C.C., Millar,A.H. and Ecker,J.R. (2008) Highly integrated single-base resolution maps of the epigenome in *Arabidopsis*. *Cell*, **133**, 523–536.
65. Sanchez,D.H. and Paszkowski,J. (2014) Heat-induced release of epigenetic silencing reveals the concealed role of an imprinted plant gene. *PLoS Genet.*, **10**, e1004806.
66. Vu,T.M., Nakamura,M., Calarco,J.P., Susaki,D., Lim,P.Q., Kinoshita,T., Higashiyama,T., Martienssen,R.A. and Berger,F. (2013) RNA-directed DNA methylation regulates parental genomic imprinting at several loci in *Arabidopsis*. *Development*, **140**, 2953–2960.
67. Yao,Y. and Kovalchuk,I. (2018) Exposure to zebularine and 5-azaC triggers microsatellite instability in the exposed *Arabidopsis thaliana* plants and their progeny. *Biocatal. Agric. Biotechnol.*, **13**, 38–45.
68. Jones,M.A., Covington,M.F., DiTacchio,L., Vollmers,C., Panda,S. and Harmer,S.L. (2010) Jumonji domain protein JMJD5 functions in both the plant and human circadian systems. *Proc. Natl. Acad. Sci. U.S.A.*, **107**, 21623–21628.
69. Nusinow,D.A., Helfer,A., Hamilton,E.E., King,J.J., Imaizumi,T., Schultz,T.F., Farre,E.M. and Kay,S.A. (2011) The ELF4-ELF3-LUX complex links the circadian clock to diurnal control of hypocotyl growth. *Nature*, **475**, 398–402.
70. Źoltowski,B.D. and Imaizumi,T. (2014) Structure and function of the ZTL/FKF1/LKP2 Group Proteins in *Arabidopsis*. *Enzymes*, **35**, 213–239.
71. Somers,D.E., Kim,W.Y. and Geng,R.S. (2004) The F-box protein ZEITLUPE confers dosage-dependent control on the circadian clock, photomorphogenesis, and flowering time. *Plant Cell*, **16**, 769–782.
72. Schmitz,R.J. and Ecker,J.R. (2012) Epigenetic and epigenomic variation in *Arabidopsis thaliana*. *Trends Plant Sci.*, **17**, 149–154.
73. Dubin,M.J., Zhang,P., Meng,D., Remigereau,M.S., Osborne,E.J., Paolo Casale,F., Drewe,P., Kahles,A., Jean,G., Vilhjálmsson,B. *et al.* (2015) DNA methylation in *Arabidopsis* has a genetic basis and shows evidence of local adaptation. *eLife*, **4**, e05255.
74. Kawakatsu,T., Huang,S.C., Jupe,F., Sasaki,E., Schmitz,R.J., Urich,M.A., Castanon,R., Nery,J.R., Barragan,C., He,Y. *et al.* (2016) Epigenomic diversity in a global collection of *Arabidopsis thaliana* accessions. *Cell*, **166**, 492–505.
75. Webb,A.A.R., Seki,M., Satake,A. and Caldana,C. (2019) Continuous dynamic adjustment of the plant circadian oscillator. *Nat. Commun.*, **10**, 550.
76. Baudry,A., Ito,S., Song,Y.H., Strait,A.A., Kiba,T., Lu,S., Henriques,R., Pruneda-Paz,J.L., Chua,N.H., Tobin,E.M. *et al.* (2010) F-box proteins FKF1 and LKP2 act in concert with ZEITLUPE to control *Arabidopsis* clock progression. *Plant Cell*, **22**, 606–622.
77. Nozue,K., Covington,M.F., Duek,P.D., Lorrain,S., Fankhauser,C., Harmer,S.L. and Maloof,J.N. (2007) Rhythmic growth explained by coincidence between internal and external cues. *Nature*, **448**, 358–361.
78. Soy,J., Leivar,P., Gonzalez-Schain,N., Martin,G., Diaz,C., Sentandreu,M., Al-Sady,B., Quail,P.H. and Monte,E. (2016) Molecular convergence of clock and photosensory pathways through PIF3-TOC1 interaction and co-occupancy of target promoters. *Proc. Natl. Acad. Sci. U.S.A.*, **113**, 4870–4875.
79. Zhu,J.Y., Oh,E., Wang,T. and Wang,Z.Y. (2016) TOC1-PIF4 interaction mediates the circadian gating of thermoresponsive growth in *Arabidopsis*. *Nat. Commun.*, **7**, 13692.
80. Martin,G., Rovira,A., Veciana,N., Soy,J., Toledo-Ortiz,G., Gommers,C.M.M., Boix,M., Henriques,R., Minguez,E.G., Alabadi,D. *et al.* (2018) Circadian waves of transcriptional repression shape PIF-Regulated photoperiod-responsive growth in *Arabidopsis*. *Curr. Biol.*, **28**, 311–318.
81. Hsieh,T.F., Shin,J.Y., Uzawa,R., Silva,P., Cohen,S., Bauer,M.J., Hashimoto,M., Kirkbride,R.C., Harada,J.J., Zilberman,D. *et al.* (2011) Regulation of imprinted gene expression in *Arabidopsis* endosperm. *Proc. Natl. Acad. Sci. U.S.A.*, **108**, 1755–1762.
82. Yang,R., He,L., Huang,H., Zhu,J.K., Lozano-Duran,R. and Zhang,H. (2020) RNA-directed DNA methylation has an important developmental function in *Arabidopsis* that is masked by the chromatin remodeler PICKLE. *J. Integr. Plant Biol.*, **62**, 1647–1652.
83. Kuroda,H., Yanagawa,Y., Takahashi,N., Horii,Y. and Matsui,M. (2012) A comprehensive analysis of interaction and localization of *Arabidopsis* SKP1-like (ASK) and F-box (FBX) proteins. *PLoS One*, **7**, e50009.
84. Shi,H., Liu,R., Xue,C., Shen,X., Wei,N., Deng,Xing W. and Zhong,S. (2016) Seedlings transduce the depth and mechanical pressure of covering soil using COP1 and ethylene to regulate EBF1/EBF2 for soil emergence. *Curr. Biol.*, **26**, 139–149.
85. Azzi,A., Evans,J.A., Leise,T., Myung,J., Takumi,T., Davidson,A.J. and Brown,S.A. (2017) Network dynamics mediate circadian clock plasticity. *Neuron*, **93**, 441–450.
86. Azzi,A., Dallmann,R., Casserly,A., Rehrauer,H., Patrignani,A., Maier,B., Kramer,A. and Brown,S.A. (2014) Circadian behavior is light-reprogrammed by plastic DNA methylation. *Nat. neurosci.*, **17**, 377–382.
87. Field,A.E., Robertson,N.A., Wang,T., Havas,A., Ideker,T. and Adams,P.D. (2018) DNA methylation clocks in aging: categories, causes, and consequences. *Mol. Cell*, **71**, 882–895.
88. Joska,T.M., Zaman,R. and Belden,W.J. (2014) Regulated DNA methylation and the circadian clock: implications in cancer. *Biology (Basel)*, **3**, 560–577.